

PB83-159764

REPORT NO.
UCB/EERC-82/18
OCTOBER 1982

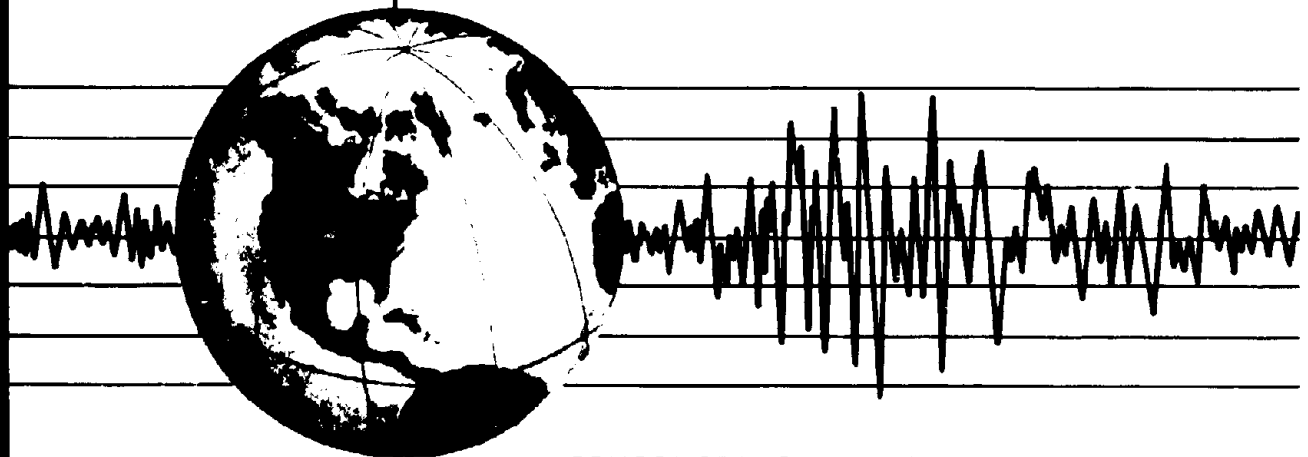
EARTHQUAKE ENGINEERING RESEARCH CENTER

MECHANICAL BEHAVIOR OF SHEAR WALL VERTICAL BOUNDARY MEMBERS: AN EXPERIMENTAL INVESTIGATION

by

MARYANN T. WAGNER
VITELMO V. BERTERO

Report to National Science Foundation



COLLEGE OF ENGINEERING

UNIVERSITY OF CALIFORNIA · Berkeley, California

REPRODUCED BY
NATIONAL TECHNICAL
INFORMATION SERVICE
U.S. DEPARTMENT OF COMMERCE
SPRINGFIELD, VA. 22161

For sale by the National Technical Information Service, U.S. Department of Commerce, Springfield, Virginia 22161.

See back of report for up to date listing of EERC reports.

DISCLAIMER

Any opinions, findings, and conclusions or recommendations expressed in this publication are those of the authors and do not necessarily reflect the views of the National Science Foundation or the Earthquake Engineering Research Center, University of California, Berkeley

REPORT DOCUMENTATION PAGE		1. REPORT NO. NCF/CEE-82067	2.	3. Recipient's Accession No. PB83 159764	
4. Title and Subtitle Mechanical Behavior of Shear Wall Vertical Boundary Members: An Experimental Investigation				5. Report Date October 1982	
7. Author(s) Maryann T. Wagner and Vitelmo V. Bertero				6.	
9. Performing Organization Name and Address Earthquake Engineering Research Center University of California, Berkeley 47th Street & Hoffman Blvd. Richmond, Calif. 94804				8. Performing Organization Rept. No. UCB/EERC-82/18	
12. Sponsoring Organization Name and Address National Science Foundation 1800 G. Street, N.W. Washington, D.C. 20550				10. Project/Task/Work Unit No.	
11. Contract(C) or Grant(G) No. (C) (G) PFR-7908984				13. Type of Report & Period Covered	
14.				15. Supplementary Notes	
16. Abstract (Limit: 200 words) An experimental program has been formulated to examine the behavior of confined edge members in reinforced concrete wall systems subjected to seismic excitations. This report describes the design and construction of the testing facility required to conduct such a program and discusses the first series of experiments and results. Eight specially shaped concrete specimens were tested to assess the mechanical characteristics of edge members. These specimens were designed to simulate one-third scale models of the edge members in a prototype 15-story, barbell-shaped wall. Four of the specimens were cast with circular spiral reinforcement while the remainder were unreinforced. None of the specimens were longitudinally reinforced. Both monotonic and cyclic shear loading were applied in combination with axial forces to the study of both monotonic and hysteretic responses of the specimens to shear loading. The effect of transverse cracks, whose widths were axially restrained, on both of the above responses, was also investigated. Experimental results indicated that high compressive forces lead to high shear resistance accompanied by large shear stiffness. The desirability of avoiding the formation of wide cracks that remain open became apparent. Recommendations are given for further research.					
17. Document Analysis					
a. Descriptors					
b. Identifiers/Open-Ended Terms					
c. COSATI Field/Group					
18. Availability Statement: Release Unlimited			19. Security Class (This Report)		21. No. of Pages 75
			20. Security Class (This Page)		22. Price

MECHANICAL BEHAVIOR OF SHEAR WALL
VERTICAL BOUNDARY MEMBERS:
AN EXPERIMENTAL INVESTIGATION

by

Maryann T. Wagner
Structural Designer
H. J. Degenkolb & Associates
Formerly Graduate Student
University of California, Berkeley

Vitelmo V. Bertero
Professor of Civil Engineering
University of California, Berkeley

Report to Sponsor:
National Science Foundation

Report No. UCB/EERC-82/18
Earthquake Engineering Research Center
College of Engineering
University of California
Berkeley, California

October 1982

ABSTRACT

An experimental program has been formulated to examine the behavior of confined edge members in reinforced concrete wall systems subjected to seismic excitations. This report describes the design and construction of the testing facility required to conduct such a program and discusses the first series of experiments and results.

Eight specially shaped concrete specimens were tested to assess the mechanical characteristics of edge members. These specimens were designed to simulate one-third scale models of the edge members in a prototype 15-story, barbell-shaped wall. Four of the specimens were cast with circular spiral reinforcement while the remainder were unreinforced. None of the specimens were longitudinally reinforced.

Both monotonic and cyclic shear loading were applied in combination with axial forces to the study of both monotonic and hysteretic responses of the specimens to shear loading. The effect of transverse cracks, whose widths were axially restrained, on both of the above responses, was also investigated.

Experimental results indicated that high compressive forces lead to high shear resistance accompanied by large shear stiffness. The desirability of avoiding the formation of wide cracks that remain open became apparent.

Recommendations are given for further research.

ACKNOWLEDGEMENTS

This report is based on the Master of Engineering thesis written by M. T. Wagner under the direct supervision of Professor Vitelmo V. Bertero. The valuable insights and advice provided by Professor S. A. Mahin and Dr. A. E. Aktan are gratefully acknowledged.

The research reported herein was sponsored by the National Science Foundation under Grant No. PFR-7908984, Subproject No. 0-22002. The financial support provided by the Foundation is most appreciated. The opinions, discussions, findings, conclusions, and recommendations presented herein are those of the authors and do not necessarily reflect the views of the National Science Foundation.

The tests were conducted in the Structural Engineering Laboratory of the Department of Civil Engineering, University of California, Berkeley. The authors would like to express their thanks to A. D. Lawrence, M. Pitrola, H. Williams, and B. Pierce for their roles in setting up and carrying out the experiments. Their help and cooperation were invaluable. The authors would also like to express their appreciation to D. Clyde for his assistance during testing, to R. Steele for drafting the figures, and to S. Gardner for overseeing the manuscript publication.

TABLE OF CONTENTS

	<u>Page</u>
ABSTRACT	iii
ACKNOWLEDGEMENTS	v
TABLE OF CONTENTS	vii
LIST OF TABLES	ix
LIST OF FIGURES	xi
LIST OF NOTATION	xiii
1. INTRODUCTION	1
1.1 General Remarks	1
1.2 Objectives and Scope	2
2. TEST SPECIMENS	5
2.1 Selection of Test Specimens	5
2.1.1 Scale	5
2.1.2 Basic Subassemblage	5
2.2 Materials	6
2.2.1 Concrete	6
2.2.2 Steel	7
2.3 Fabrication and Casting of Specimens	7
3. EXPERIMENTAL SETUP AND TESTING PROCEDURE	9
3.1 General Setup	9
3.2 Testing Frame	9
3.3 Loading Devices	9
3.3.1 Shear Loading System	9
3.3.2 Axial Loading System	10
3.4 Ancillary Apparatus	12
3.5 Specimen Instrumentation	12
3.5.1 Measurement of Shear Deformations	12
3.5.2 Measurement of Axial Deformations	14

Table of Contents (cont'd)	<u>Page</u>
3.5.3 Measurement of Spiral Strain	14
3.6 Data Acquisition System	14
3.7 Testing Procedure and Loading Sequence	15
3.8 Performance of Testing Facility	15
4. TEST RESULTS AND THEIR EVALUATION	17
4.1 General Remarks	17
4.2 Monotonic Behavior	17
4.2.1 Under Constant Axial Load	17
4.2.2 Under Constant Crack Width	20
4.3 Hysteretic Behavior	21
4.3.1 Under Constant Axial Load	21
4.3.2 Under Constant Crack Width	22
5. APPLICATION OF EXPERIMENTAL RESULTS TO SHEAR WALL BEHAVIOR .	25
5.1 General	25
5.2 Monotonic Loading	25
5.3 "Elastic" Cycling	27
5.4 Inelastic Cycling	29
6. CONCLUSIONS AND RECOMMENDATIONS	31
6.1 Conclusions	31
6.1.1 Performance of Testing Facility	31
6.1.2 Behavior of Tested Edge Member Specimens	31
6.1.3 Behavior of Barbell-Shaped Isolated Shear Walls	32
6.2 Recommendations for Future Research	33
6.2.1 Testing Facility	33
6.2.2 Test Specimen	33
REFERENCES	35
TABLES	37
FIGURES	45

LIST OF TABLES

<u>Table</u>	<u>Page</u>
2.1 Concrete Mix	39
2.2 Mechanical Characteristics of Concrete	40
3.1 Axial Loads Applied During Testing	41
4.1 Comparison of Experimental and Theoretical Shear Moduli . . .	42
4.2 Comparison of Experimental and Theoretical Shear Strengths of Initially Uncracked Specimens	43

LIST OF FIGURES

<u>Figure</u>	<u>Page</u>
1.1 Shear Wall Failure Modes	47
2.1 Test Specimen Geometry	48
2.2 Concrete Stress-Strain Diagram	48
2.3 Stress-Strain Relationship of the #2 Reinforcing Bar Used for the Spiral	49
2.4 Formwork Assemblage Procedure	50
2.5 Conduit Support Detail	53
2.6 Placement of Instrumentation Fixtures	53
3.1 Experimental Setup	54
3.2 Shear Reaction Bracing	55
3.3 Axial Loading System	56
3.4 Axial Loading Apparatus	57
3.5 Specimen, Confining Plates, and Load Transfer Plates	58
3.6 Specimen Shear Deformations	58
3.7 Shear Deformation Instrumentation - Scheme 1	59
3.8 Shear Deformation Instrumentation - Scheme 2	59
3.9 Placement of Shear Displacement Instrumentation Mounted on Steel Plates	60
3.10 Placement of Axial Deformation Instrumentation	60
3.11 Typical Loading Program	60
4.1 Comparison of Monotonic $v-\delta_v$ Diagrams, Specimens S1C2 & S1C3	61
4.2 Comparison of Monotonic $v-\delta_v$ Diagrams, Specimens S1U1 & S1C4	61
4.3 Relationship of Initial Shear Strength to Normal Stress . .	62
4.4 Observed Failure Modes	62
4.5 Typical Cyclic $v-\delta_v$ Diagram	63

List of Figures (cont'd)	<u>Page</u>
4.6 Frictional Shear Resistance Versus Normal Stress Diagram . .	63
4.7 Axial Shortening Versus Shear Displacement Diagrams, Specimens S1C3 & S1C4	64
4.8 γ - δ_v and p - δ_v Diagrams for Specimen S1C4 Cycled under a Constant Average Crack Width of 0.02 in.	65

LIST OF NOTATION

A_g	gross cross-sectional area
c	cohesive strength
E_c	elastic modulus of concrete
f'_c	compressive strength of concrete
f_r	modulus of rupture of concrete
G	shear modulus
h	core height
p	axial stress
v	shear stress
v_f	frictional shear stress
δ_v	shear displacement (Fig. 3.6)
γ	shear angle
λ	form factor for shear
ν	Poisson's ratio
ϵ_o	concrete strain at maximum stress of 6-in. x 12-in. standard cylinder

1. INTRODUCTION

1.1 General Remarks

Efficient design of earthquake-resistant structures requires the use of a structural system capable of providing stiffness, strength and stable hysteretic behavior with large energy dissipation capacity. Post-earthquake damage observations [1,2] and experimental investigations [3 - 7] indicate that these characteristics can be met with properly designed reinforced concrete structural wall systems.

The barbell shape has been found to be a particularly advantageous shear wall cross section for use in seismic-resistant design. The barbell configuration results from a wall panel between two edge members greater in thickness than the panel. This geometry enables convenient placement of flexural steel for increased flexural strength and curvature ductility and increases the out-of-plane wall stiffness, reducing the tendency for lateral instability. In addition, by selecting edge members with circular or square cross section, confinement of the concrete and lateral restraint of the longitudinal reinforcement in the edge members is facilitated. Such advantages are not as easily realized in rectangular walls where the edge members are developed within the thickness of the wall panel. Barbell-shaped walls consequently exhibit increased rotation capacity, improved restraint against construction joint slip, and increased shear strength and deformation capacity.

Circular spiral steel can be efficiently used as transverse confining reinforcement in the edge members. The ease of providing small spiral pitch and uniform radial confinement makes its use particularly attractive. Strong and ductile edge members result from this confinement.

The addition of well-confined edge members significantly improves the seismic-resistant behavior of reinforced concrete walls. This becomes evident from consideration of the possible failure mechanisms of walls subjected to seismic actions (Fig. 1.1). An efficient seismic-resistant design requires the shear-types of failure to be avoided or delayed until sufficient energy is dissipated through flexural yielding. An analysis of the different shear mechanisms clearly indicates that because of their required confinement the shear wall vertical boundary members (edge members) can act as large diameter dowels or short ductile columns, thus they can be a significant factor in achieving the desired response of barbell-shaped walls. Unfortunately, there is a lack of data regarding the behavior of confined concrete subjected to high shear and axial loads, and consequently, it is impossible to accurately predict the response of these edge members to these extreme combined loading conditions. This in turn prohibits an understanding of wall panel and edge member interaction. To provide the required information, it was decided to investigate the behavior of these confined edge members.

1.2 Objectives and Scope

The objective of this study is to gain an understanding of edge member behavior under seismic-type excitations. A test program has been designed to experimentally examine the behavior of confined edge members. The ultimate goal is to use the information of this investigation to develop a rational basis for designing barbell-shaped walls against the effects of severe earthquake ground motions.

The scope of this report is limited to the initial phase of the experimental program which consisted of the design and construction of the testing facility and the first series of experiments. Only edge members confined with circular spiral reinforcement were investigated in this test series. The general experimental setup and testing procedure as well as the test results and conclusions from the first set of specimens are presented herein.

2. TEST SPECIMENS

2.1 Selection of Test Specimens

The simplest test specimen capable of duplicating prototype edge member behavior was sought. In addition, a scale suitable for accurately modeling this behavior was required. The factors governing the selection of both specimen form and scale are described below.

2.1.1 Scale

Difficulties in accurately reproducing prototype behavior on small scale models prompted the use of a test specimen on the largest feasible scale. It was also desired to correlate test results with one-third scale coupled shear wall tests performed at the University of California, Berkeley [8]. Since available testing capacities prohibited the use of a full-size specimen, a model of the same scale and configuration as that used in the coupled shear wall tests was adopted.

2.1.2 Basic Subassemblage

Several factors governed the selection of a subassemblage. First, tests have shown that crushing of edge member cover has little effect on the strength and ductility of barbell shear walls [4]. Thus, only the core was modeled. A nine-inch (229 mm) diameter core was used for the test specimen. Second, shear wall failure resulting from diagonal tension or sliding shear tends to concentrate inelastic behavior in the edge member over a limited height. To investigate the response of edge members under such conditions, the core height was selected as one of the main parameters to be studied. For the series of tests reported herein, the core height was one inch (25.4 mm). To ensure failure over this height, the specimen was specially shaped and strengthened above

and below the core by post-tensioning. A square section was adopted at these locations to facilitate post-tensioning of the concrete and loading of the specimen. Figure 2.1 illustrates the test specimen geometry.

To compare and contrast the behavior of confined and unconfined edge members, half of the test specimens were confined with 1/4-inch (6.4 mm) diameter spiral at 3/4-inch (19.1 mm) pitch. The selected pitch permitted one complete revolution of the spiral within the 1-inch (25.4 mm) core height.

Longitudinal steel was omitted from all specimens in this test series to isolate behavior of the concrete.

2.2 Materials

2.2.1 Concrete

The mix design used in this study was based on a specified 28-day strength of 5000 psi (34.5 MPa). Portland cement Type I, coarse and fine sand, and 3/8-inch (9.5 mm) maximum size aggregate constituted the selected mix. The same mix design was used for all specimens; minor modifications of the water-cement ratio adjusted the slump at the time of casting. Table 2.1 shows the mix design.

Although 5000 psi 28-day strength was specified, cylinder strengths at 28 days ranged from 4669 to 5199 psi. On the days of testing (48-69 days after casting) average cylinder strengths ranged from 5022 to 5330 psi. In addition to compression tests, splitting tensile and flexural (beam) tests were performed on concrete samples for each specimen. The results of these tests are summarized in Table 2.2.

Additional 6 x 12-in. cylinders were tested for four of the eight specimens to evaluate the elastic modulus of concrete, E_c . A stress-strain

curve typical of those obtained is given in Figure 2.2. The average secant modulus at $0.45 f_c$ was 2770 ksi (19,100 MPa). Experimental secant moduli and those computed from the ACI equation: $E_c = 57,000 \sqrt{f'_c}$ [9] are compared in Table 2.2. In all cases the experimental moduli are considerably lower than the ACI theoretical values. Results obtained by other researchers suggest that the low experimental values were a consequence of the small aggregate size used [10].

Poisson's ratio, ν , was also measured experimentally in one of the cylinder tests. A value of 0.15 was obtained at $0.45 f'_c$.

2.2.2 Steel

Deformed #2 steel bars with a nominal diameter of 0.25-in. (6.4 mm) were used as circular spiral reinforcement. Figure 2.3 shows an average stress-strain diagram for the bars. The steel yielded at a nominal stress of 69 ksi (476 MPa) and attained a maximum stress of 92 ksi (634 MPa). Rupture of the bar occurred at 24 percent elongation.

2.3 Fabrication and Casting of Specimens

A total of 8 specimens were fabricated. They were cast four at a time in a vertical position. Reusable wood forms made of high density overlay plywood were used. Figure 2.4 illustrates the procedure followed in assembling the formwork.

Special care was taken in designing the formwork to be used to cast the core test region (Fig. 2.1). The selected form was radially tapered from a 2-inch (5.08 mm) thickness at the outside of the specimen to 1-inch (2.54 mm) at the core. The taper reduced the possibility of trapping air in the bottom half of the specimen while casting, facilitated removal of the form after casting, and reduced the stress concentration between the core and the post-tensioned concrete above and below it. Modification of this formwork piece

permits reuse of the forms in future tests for specimens with cores up to 10 inches (254 mm) in height.

High strength A490 threaded rod was used to provide the desired post-tensioning in the concrete adjacent to the core. Conduits were cast in the specimens to provide ducts for the threaded rods. The conduits were held in place as detailed in Fig. 2.5. Wooden dowels glued and nailed to the inside of the forms positioned the conduits within the formwork. Closed-cell ethafoam was used to seal the conduit from the wet concrete.

Steel rods 1/4-inch (6.4 mm) in diameter were cast in each specimen to attach instrumentation. The arrangement of these fixtures is illustrated in Fig. 2.6.

The four confined specimens had identical spiral and pitch. Three-quarter inch spiral pitch was maintained with tie wire positioned at third points along the circumference of the spiral. Anchorage of the spiral was provided by extending it approximately 5 inches (127 mm) above and below the core with two additional turns at each end.

Casting was facilitated by the use of a high frequency hand vibrator. After casting, the specimens were covered with wet burlap and plastic for seven days. The forms were stripped on the seventh day. The specimens were stored in the laboratory at approximately 70°F (21°C) until the dates of testing. The ages of the specimens at the times of testing ranged from 48 to 69 days.

3. EXPERIMENTAL SETUP AND TESTING PROCEDURE

3.1 General Setup

The experimental setup, including test specimen and testing facility, is shown in Fig. 3.1. As illustrated, the specimen was tested in a vertical position. The testing facility consisted of a testing frame, loading devices, ancillary apparatus, instrumentation, and a data acquisition system. Each is described below.

3.2 Testing Frame

The testing frame was fabricated from structural steel members. It was designed to resist forces of 600 kips (2670 kN) axial compression, 200 kips (890 kN) axial tension, and 235 kips (1050 kN) shear on the specimen. A horizontally oriented reaction frame resisted the shear force applied to the specimen. Figure 3.2 illustrates this framework. Axial forces were resisted by a cross-head (Fig. 3.1) consisting of large girders arranged in a grid. The cross-head was supported by four columns anchored by prestressed rods to the laboratory floor. A beam and two additional columns supported the weight of the lateral loading jack.

3.3 Loading Devices

The loads applied to a typical specimen included both axial and shear loads. The loading systems used for each load type were independent of one another. Each is described subsequently.

3.3.1 Shear Loading System

The shear load was applied with a double-acting hydraulic jack. Operating at 3000 psi (20.7 MPa) oil pressure, its maximum load capacity is 235 kips (1050 kN) push and 176 kips (780 kN) pull. The jack has a

stroke of 24 inches (610 mm). The force applied by this jack was directly measured by a 200 kip (890 kN) capacity load cell connected between the jack cylinder and the test specimen.

The shear jack was operated by an electrically-controlled servo-valve. The servo-valve was controlled by an MTS controller. The electrical output from the load cell measuring the shear force and from an LVDT mounted on the jack measuring the movement of the ram were used as input to the controller transducer conditioners. After receiving these signals, the feedback selector determined which would be used as input to the servo-controller. In this way, the shear loading jack could be operated under load or displacement control. To improve the accuracy of the measurements taken and to avoid the danger of a sudden collapse resulting from deformation softening, displacement control was used exclusively in all tests.

3.3.2 Axial Loading System

Lack of experimental data regarding the behavior of concrete subjected to shear and axial tension led to the development of an axial loading system with the capability of applying both tension and compression. An existing 600-kip (2670 kN) capacity single-acting hydraulic jack was capable of applying the required compressive force. The jack has a stroke of 6 inches (152 mm) and was manually controlled with an air-operated booster pump. A compression transducer was mounted directly on top of the jack. The jack was supported by a heavy movable cart which rode on large roller bearings on ground rails, permitting unrestrained lateral displacement of the bottom half of the specimen relative to the top.

To modify this system for applying tension, a loading platform consisting of a grid of welded heavy structural steel members was used. A

pin and clevis connected the platform to the axial jack. Four 1-1/8-in. (28.6 mm) diameter prestressing rods were connected to the platform and inserted through tie-down holes in the laboratory floor slab. The platform, rods, and jack are illustrated in Fig. 3.3. Beneath the floor, the rods were connected in pairs by heavy box section beams. A 200-kip (890 kN) capacity jack was placed between each beam and the floor slab. This setup is shown in Fig. 3.4.

A 50-kip (222 kN) capacity load cell was connected to each rod on top of the loading platform. The net force on the specimen was equal to the difference of the forces measured by the load cells on the rods and the axial jack. The signals from the five axial load cells were sent to an analog computer which produced a single signal of the net axial force on the specimen.

This loading system provided the capability of applying tension, compression or alternating axial loads to the specimen. To apply compression, the rods were pretensioned against the axial jack for stability. Each rod was loaded to approximately 5 kips (22 kN). A self-equilibrated system consisting of the rods, jack, loading platform and laboratory floor results prior to connection of the specimen. After connection, the axial jack was used to apply the desired compression.

To apply tension, the specimen was first connected to the axial loading system and subjected to a compressive force of about 1 kip (4.4 kN). The rods were subsequently tensioned to a total force in excess of the axial load desired on the specimen during testing. Retraction of the axial jack cylinder produced a net tensile force on the specimen.

3.4 Ancillary Apparatus

Steel plates encased the specimen and were part of the post-tensioning apparatus providing biaxial confinement of the concrete adjacent to the core. The plates on the east and west faces of the specimen were also used to transfer the shear force to the specimen. These were connected to "ear-shaped" steel plates which were in turn attached to the shear loading jack at the west side and lateral reaction bracing at the east. Figure 3.5 illustrates the apparatus.

Proper alignment of the plates permitted application of pure shear through the mid-height of the core. The plates were designed to allow for future modifications in the test specimen so that core heights up to 10 inches (254 mm) can be tested with shear through the center by repositioning of the steel plates.

3.5 Specimen Instrumentation

3.5.1 Measurement of Shear Deformations

Shearing deformations are typically given in terms of the angular change between two faces of an element, γ . To evaluate the shear deformation of the test core, the relative displacement of the top and bottom of the core in the direction of the applied shear force was measured. Figure 3.6 illustrates the shear deformation quantities.

The expected magnitude of the relative elastic shear displacement was on the order of 0.001 inch (0.025 mm), however, large deformation behavior was also of interest; therefore, an accurate study of the complete shear deformation response required instrumentation sensitive over a large range. Linear variable differential transformers, LVDT's, were selected for use because of the sensitivity they could provide.

It was impossible to utilize the test frame itself or an auxiliary frame as a reference from which to take absolute measurements of the displacements of the top and bottom of the core as the slightest movement of either reference would invalidate measurements taken in the elastic range. In addition, the geometry of the setup made it practically impossible to devise a reliable referencing scheme since this required relative displacement measurements to be taken directly.

The 1-inch (25.4 mm) core height limited the space available for instrumentation and difficulties in reliably mounting the LVDT's within this space prompted the use of two different schemes to measure the average relative shear displacement of the test specimen.

The first arrangement is illustrated in Fig. 3.7 and consisted of: 1) An LVDT holder, designed to slip over the 1/4-inch diameter pin cast in the top half of the specimen; and 2) An LVDT, mounted in the holder and measuring the relative shear displacement against the bar cast in the bottom half of the specimen (two LVDT's with ranges of ± 0.1 inch (± 2.54 mm) were mounted in this fashion).

A second system measured the shear displacement at the center of the specimen. Figure 3.8 illustrates this instrumentation setup, which consisted of: 1) Two 1/4-inch diameter steel bars cast parallel to each other directly above and below the test section; 2) LVDT holders, connected to opposite ends of the top bar within 1/2 inch (12.7 mm) of the core; 3) Two small plates, fabricated to fit on the bottom bar; and 4) LVDT's with ranges of ± 0.1 inch mounted in the holders and measuring against the plates. The average of these readings provided a second measure of the shear displacement.

After several cycles of loading, the integrity of the core is reduced by cracking and/or crushing of the concrete and the reliability of the

measurements obtained using the schemes presented above is reduced once this stage is reached. Alternate schemes were developed to circumvent this problem. Two LVDT's with ± 0.1 -inch (± 2.54 -mm) range were mounted on the steel plates post-tensioned to the specimens to measure the relative displacement of the steel plates.

Two additional LVDT's with ± 1 -inch (± 25.4 -mm) range were also mounted on the steel plates, illustrated in Fig. 3.9. These instruments provided data regarding the specimen response to large displacement cyclic shear loading. At large displacements, the ± 0.1 -inch (± 2.54 -mm) LVDT's were disengaged.

3.5.2 Measurement of Axial Deformations

The axial deformation of the 1-inch (25.4-mm) core was measured with two LVDT's, having ranges of $\pm 1/2$ inch (± 12.7 mm), mounted in holders attached to the steel plates post-tensioned to the specimen. The LVDT's measured directly against specially prepared surfaces on the plates opposite them. Figure 3.10 illustrates the placement of this instrumentation.

3.5.3 Measurement of Spiral Strain

The confining pressure on the core is directly proportional to the stress in the spiral. To measure the associated spiral strain, two weldable strain gages were attached at diametrically opposed points on the outside of the spiral within the exposed test core.

3.6 Data Acquisition System

All transducers used for testing were read at selected stages of the test directly through a high-speed data acquisition system. Two X-Y-Y' recorders were used during testing to provide continuous plots

of the shear force versus axial load, axial displacement, shear displacement and feedback displacement.

3.7 Testing Procedure and Loading Sequence

At the commencement of testing, a predetermined axial load was applied to each specimen. A summary of the applied axial loads is given in Table 3.1. The selected stresses of $0.45 f'_c$ and $0.7 f'_c$ correspond to static and dynamic service level stresses, respectively. In six of the eight specimens tested, the prescribed axial load was manually held constant with an air pump. The shear force versus axial load recorder plot served as a guide for maintaining a constant axial load. Shear displacements were generally applied according to the loading history shown in Fig. 3.11.

After specimens S1U4 and S1C4 were initially cracked, the crack width rather than axial load was maintained constant for the duration of the test by making manual adjustments of the axial load according to the recorder plot of shear force versus axial displacement.

3.8 Performance of Testing Facility

In general, the performance of the testing facility was excellent. Only minor problems arose during testing of the first specimens which led to the introduction of slight modifications. Several of the bolted friction connections slipped during application of the shear force, so to eliminate the resultant "noise" in the test data, some of the connections were welded. Rotation of the bottom half of the specimen about the pin and clevis connection directly beneath it was also noted and screw jacks were positioned in the connection to restrain its rotational freedom.

After the modifications mentioned, the testing facility was proven to be capable of applying a shear force of 212 k (943 kN), which is close to the maximum load capacity of the jack used for such a purpose [235 kips (1050 kN)].

4. TEST RESULTS AND THEIR EVALUATION

4.1 General Remarks

To facilitate the presentation of experimental results, the discussion is divided into two parts. Those results obtained under monotonically increasing displacements are discussed under the heading of Monotonic Behavior. The results obtained under repeated cycles of deformation reversals are presented under the denomination of Hysteretic Behavior.

4.2 Monotonic Behavior

4.2.1 Under Constant Axial Load

Initial Stiffness. The initial shear stress, v (obtained dividing the total applied shear load by the gross area of the core), versus shear deflection, δ_v , response was linear for all specimens tested under constant axial load, as can be seen from the plots of v vs. δ_v for four of the specimens shown in Figs. 4.1 and 4.2. A comparison of these plots indicates that the initial tangent stiffness is related to the axial load and a trend of increasing stiffness with increasing compressive normal stress is suggested.

The dependency of initial stiffness on normal stress is contrary to the concept of linear elastic behavior. Although concrete is not a linear elastic material, its behavior under low stress levels can be approximated as such and its elastic modulus, E_c , and Poisson's ratio, ν , remain nearly constant below a stress level of approximately $0.45 f'_c$, consequently, the initial shear stiffness should remain constant according to the equation:

$$G = \frac{E_c}{2(1 + \nu)}$$

Average experimental values for E_c and ν yield an average theoretical shear modulus of 1200 ksi (8274 MPa). Experimentally derived shear

moduli are computed from the equation:

$$G = \frac{\lambda v}{\gamma}$$

where

λ = form factor ($\frac{10}{9}$ for circular cross section)

v = shear stress

γ = shear angle (rad)

Experimental and theoretical shear moduli are compared in Table 4.1. In all cases the experimental moduli are significantly less than the value predicted by linear elastic theory. This inconsistency between the measured and theoretically computed shear moduli can be attributed to several factors. Of particular significance is microcracking initiated during curing of the specimens which influences the linearity of the v - δ_v response and reduces the measured stiffness. More extensive cracking within the core resulting from handling of the specimens is also a possibility which must be acknowledged. Cracking would result in a significantly reduced initial stiffness. Additionally, the flexibility of the conduits cast in the specimens near the test section should be considered as a possible source of deformation tending to decrease experimental shear stiffnesses.

The magnitudes of the elastic shear displacements were near the level of electronic noise in the data acquisition system in some cases. The loss of significance which results coupled with the uncertain internal state of deformation require, first, that the results presented for the linear elastic range of behavior be considered approximate, and second, that this problem be further investigated.

Initial Strength. The average initial shear strengths of the specimens based on gross cross-sectional properties are listed in Table 4.2. The experimental strengths are compared with shear strengths obtained using analytically derived expressions. In most cases the experimental strengths exceeded the analytical values, particularly for the specimens subjected to high axial loads. There is an extreme discrepancy between the ACI values [9] and the experimental results because the ACI equation predicts the diagonal tensile strength of concrete and not the punching shear strength associated with high axial loads. The Bresler-Pister equation [11] was also derived from experimental results where shear failure was initiated by diagonal tension cracking in the concrete.

The dependency of the experimental shear strengths on the applied normal stress is illustrated in Fig. 4.3. The general trend of the curve indicates increased shear strength with normal stress but reduced rate of increase under high axial loads. It should be noted that for simplicity the direct contribution of the spiral to the shear strength of the confined specimens was not deducted from the recorded strengths. The contribution is dependent on the precise nature of cracking in the core and the maximum possible contribution of the spiral steel to the shear strength is only 50 psi (0.34 MPa).

The nonlinear shear strength versus normal stress relationship was substantiated by observations made during testing. Three general types of failure were observed: diagonal tension, crushing, and a combination of the two. Failure under zero normal stress was sudden -- a single diagonal tension crack formed across the specimen. Under a normal stress of $0.45 f'_c$, failure was less sudden -- a zone of crushed concrete connected with diagonal cracks provided the failure surface. Under an axial stress

of $0.7 f'_c$, the first visible cracks were nearly vertical. The presence of high shear stress reduced the effective compressive strength of the concrete, resulting in a crushed zone across the entire core.

Figure 4.4 illustrates the three observed failure modes.

In general, spiral reinforcement will strengthen a concrete core by providing radial confining pressure that can also help maintain the integrity of the core by restraining the near vertical cracking observed under high axial loads. In this test series, however, little difference in strength or behavior was noted between the confined and unconfined specimens, due largely to two factors. First, the normal stress levels were not high enough to produce significant confining pressure by the spiral. The maximum spiral stress produced by the axial stress on the core was 10 ksi (69 MPa) resulting in an average peak confining pressure of 150 psi (1.0 MPa). Second, and perhaps the more important factor, was the post-tensioned concrete above and below the test core. The post-tensioning precompressed the test section prior to testing and restrained lateral expansion of the core during testing.

4.2.2 Under Constant Crack Width

Specimen S1C4 was initially loaded in shear while subjected to constant axial tension. When the maximum shear resistance was reached, a crack formed across the test section and shear loading was continued while a constant average crack width of 0.02 inch (0.51 mm) was maintained. The initial shear stiffness measured after cracking was 2200 k/in. (385 kN/mm), approximately one-eighth of the stiffness measured during initial loading of the specimen in its uncracked state. Specimen S1U4 was subjected to one cycle of shear loading with a constant average crack width of 0.05 inch (1.3 mm). An initial cracked shear stiffness of

600 k/in. (105 kN/mm) was found.

These results indicate markedly reduced stiffness for cracked edge members where crack closure is restrained.

4.3 Hysteretic Behavior

4.3.1 Under Constant Axial Load

The specimens cycled in shear while subjected to a constant axial load exhibited similar shear stress versus shear displacement relationships. A typical plot is shown in Fig. 4.5. The load-deflection behavior is characterized by initially linear response, as discussed previously, with a subsequent reduction in resistance after maximum shear strength is reached. In all cases, after two cycles of shear loading with shear displacements of approximately 0.3 inch (7.6 mm), i.e., exceeding that corresponding to maximum shear resistance, the shear resistance became nearly constant. This inelastic behavior represented frictional resistance to shear. Test results indicate that the frictional shear resistance increases linearly with normal stress. This relationship is illustrated in Fig. 4.6.

These results can be understood in terms of the Coulomb-Mohr failure theory which is expressed by the equation:

$$v = p \tan \phi + c$$

where ϕ is the internal friction angle, c is the cohesive strength, p is the normal stress, and v is the shear strength. If a fully cracked failure surface has been formed, the cohesion is zero. The equation:

$$v_f = p \tan \phi$$

fully defines the frictional shear strength in this case.

The experimentally derived internal friction angle, ϕ , was 32° . This correlates very well with the average friction angle obtained by other researchers [12].

Constant frictional resistance was attainable because axial shortening of the specimens was unrestrained. Each cycle of shear loading was accompanied by axial shortening of the specimen due to abrasion and grinding of adjacent concrete surfaces. Figure 4.7 illustrates the relationship between axial shortening and shear displacement for two specimens subjected to different axial loads. After small displacement cycles, the grinding failure was accompanied by near constant axial distortion per unit shear displacement, independent of the absolute shear displacement. Under a normal stress of $0.7 f'_c$, Specimen S1C3 exhibited an average axial displacement of 0.07 inch per inch of shear displacement; Specimen S1C4 under a normal stress of $0.3 f'_c$ shortened an average of 0.03 inch axially for each inch of shear displacement. Although sufficient data is not available to generalize these results, a direct proportionality between axial shortening and normal stress is suggested for the range of axial stresses used in this study.

4.3.2 Under Constant Crack Width

Specimen S1C4 was cycled in shear while a constant average crack width of 0.02 inch (0.51 mm) was maintained. A dramatic difference in the shear force versus shear displacement relationship was seen for this specimen. Rather than exhibiting stable hysteretic behavior, as did the specimens under constant axial load, the hysteretic load-deflection curve for this specimen showed degrading strength and stiffness, in addition, the hysteretic loops were highly pinched.

Similar test results have been found by other researchers [13]. The shear stress versus shear displacement response accompanied by the corresponding axial stress versus shear displacement relationship is shown in Fig. 4.8. The shear stress-shear deflection behavior illustrated was highly dependent on the normal forces developed during cycling. Shear resistance was proportional to the average axial stress developed over the cross section by local bearing of aggregate from adjacent crack faces.

5. APPLICATION OF EXPERIMENTAL RESULTS TO SHEAR WALL BEHAVIOR

5.1 General

The experimental results presented in Chapter 4 have limited applicability. They cannot be directly related to the strength or deformation characteristics of barbell-shaped walls because testing was limited to longitudinally unreinforced concrete. The data obtained can, however, be used to provide insight into the participation of edge members in the shear resistance of laterally loaded shear walls. The potential effect of edge members will be discussed according to the load history of isolated shear walls.

5.2 Monotonic Loading

Under low shear and axial loads, an elastic distribution of shear stress will develop across a wall. Elastic theory dictates that the shear force at this stage is resisted primarily by the wall panel, as loading increases, however, cracking in the tensile edge member and in the wall panel modifies the shear distribution. Four static shear failure modes have been observed.

Web Crushing. This failure mode is common in walls with relatively thin panels. Flexural cracking along the tensile edge of the wall propagates diagonally across the wall panel due to the presence of high shear. The shear force must be transferred across the wall through the inclined struts between these cracks which results in a small zone of high compressive stresses leading to panel splitting and/or crushing. Figure 1.1(a)(i) illustrates this failure mode.

The confined compression edge member core is generally sound when the panel crushes since the effective compressive strength of the core

is greater than the strength of the unconfined panel. At this stage, the edge members act as short columns to resist the shear and associated bending and axial forces. No experimental data has yet been collected to predict the shear strength under this situation.

Diagonal Tension. If a wall panel has not been adequately designed to resist shear or if the shear span to depth ratio is small, a sudden diagonal tension crack can form across the panel resulting in a sudden transfer of shear to the compression edge member. This failure mode is illustrated in Fig. 1.1(a)(ii).

The compression edge member ultimately fails in punching shear or diagonal tension depending on the magnitude of its axial force. The data given in Fig. 4.3 provides an estimate of the maximum concrete shear resistance of the edge member.

Sliding Shear. It is possible to conceive of shear failure due to sliding at a construction joint. A poor quality construction joint provides a plane of weakness susceptible to sliding. Figure 1.1(a)(iii) illustrates this mode of failure.

Experimental results have indicated, however, that the resistance of edge members to punching shear is very great. Large shear forces would be required to deform both edge members sufficiently to permit sliding and it is likely that the required shear force is in excess of that causing web crushing in typically proportioned barbell-shaped walls, confirming the lack of sliding shear failures observed in such walls.

Combined Diagonal Tension and Sliding Shear. Under relatively low loads it is common for a horizontal flexural crack to form near the base of a wall across the width of the panel. Sliding may occur along this crack

surface, but the strength and stiffness of the compression edge member prevents the crack from propagating into it, the lateral force on the wall is consequently permitted to increase. Excessive shear in the panel can lead to diagonal cracking. Depending on the magnitude of the axial force in the compression edge member and the arrangement of the panel cracks, failure of the edge member will result from punching shear or diagonal tension. The maximum concrete resistance of the edge member is given in Fig. 4.3.

5.3 "Elastic" Cycling

Elastic cycling of a shear wall will typically cause its edge members to crack in tension, and additionally, a horizontal flexural crack will likely form across the wall panel near the base. Since cycling is restricted to the elastic range, the longitudinal steel in the edge members will not have yielded. Cracks in the tensile edge member will (except for the effects of volumetric changes) tend to close upon load reversal. After a few small shear displacement cycles, a lower bound on the shear resistance of the concrete in the edge member will be given by the frictional resistance summarized in Fig. 4.6, however as the number of cycles increases, the concrete will abrade. An effective widening of the edge member cracks will result from the abrasion and grinding since longitudinal steel restrains the axial distortion of the concrete. The steel in the edge members resists most of the lateral force at this stage. Since the concrete within the core is generally intact and confined with closely-spaced lateral reinforcement, buckling of the longitudinal bars in the edge members will be restrained. This will permit the edge member cores to act as large dowels in resisting

shear. Experimental data must be collected to estimate this final shear strength.

Lower bound estimates of the shear strength of edge members are available from other researchers [4-6]. Tests have been performed on barbell-shaped shear wall models consisting of square edge members with cores equal in diameter, similar in concrete strength, and similar in confinement type and spacing to those used in the investigation reported herein. Pseudo-static, seismic-type excitations were applied to these wall models according to various load histories. In general, flexural cracks in the tension edge member, diagonal cracks in the wall panel, and partial crushing of the compression edge member cover preceded web crushing failure of these specimens. In one specimen which was cycled elastically and subsequently loaded monotonically to failure [4], a maximum shear force of 248 kips (1103 kN) was resisted prior to panel crushing. The loss of the panel as a significant shear resisting element caused the lateral force to suddenly drop to 180 kips (801 kN). The axial force on the compression edge member was 380 kips (1690 kN) at this stage and this edge member remained as the primary shear resisting element in the wall.

The high axial compression to which the edge member was subjected likely reduced its shear strength relative to the specimens tested under 225 kips (1000 kN), reported on in this investigation. The average of the initial shear strengths of Specimens S1U3 and S1C3 was 205 kips (910 kN). The apparent reduction in shear strength under higher axial loads correlates well with the trend suggested in Fig. 4.3.

5.4 Inelastic Cycling

Wide cracking in the tension edge member will result from yielding of the longitudinal steel therein. Upon load reversal, these cracks will remain open until comparable yielding occurs in the opposite direction. Resistance from the concrete in the edge member is available only at large displacements since the shear stiffness of concrete with a finite crack width is greatly reduced. At large displacements, however, the edge member reinforcement is capable of effectively resisting applied lateral forces.

6. CONCLUSIONS AND RECOMMENDATIONS

6.1 Conclusions

From observations made during testing and an evaluation of the experimental results obtained, several conclusions have been drawn. They are grouped into three categories. First, conclusions regarding the performance of the testing facility are presented. Second, conclusions concerning the behavior of the test specimens are given. Finally, implications relating to the overall behavior of barbell-shaped walls are listed.

6.1.1. Performance of Testing Facility

(1) The test frame has been proven to be capable of applying a shear force of 212 kips (943 kN). The design load of 235 kips (1045 kN) shear is likely attainable, but perhaps insufficient to test specimens subjected to axial stresses in excess of $0.7 f'_c$ and/or those reinforced with longitudinal steel if the height of the core is kept equal to one inch.

(2) Frictional losses in the test frame likely reduced the shear forces applied to the specimens. The magnitude of these reductions could not be measured with the given testing facility.

6.1.2 Behavior of Tested Edge Member Specimens

The specimens tested provided data on edge members subjected to axial stresses ranging from $0.02 f'_c$ tension to $0.7 f'_c$ compression. The conclusions drawn from an evaluation of the test results follow.

(1) The magnitudes of the experimental shear moduli, G , were smaller than that generally assumed.

(2) The shear strength of all specimens was sensitive to the applied normal stress. Increased axial stresses resulted in larger

shear strengths. The shear strength increased less rapidly at axial stresses above a service level of $0.45 f'_c$ when crushing preceded shear failure. Because punching shear rather than diagonal tension failure results under the combination of high axial compression and shear, the ACI equation is too conservative to predict the shear strength of edge members.

(3) When axial distortion of the specimens was unrestrained, a constant frictional resistance was obtained under cyclic shear loading. This corresponded to a concrete internal friction angle, ϕ , of approximately 32° .

(4) The monotonic behavior of cracked specimens with crack widths maintained constant during shear loading was markedly different from that of uncracked specimens tested under a constant axial load. Maximum shear resistance of the cracked specimens was attained at considerably larger displacements than for the uncracked specimens. An average crack width of 0.02 inch (0.51 mm) reduced the initial stiffness of Specimen S1C4 to one-eighth of that computed for uncracked Specimen S1U1 tested under zero axial load. The maximum shear resistance of Specimen S1C4 was only about one-tenth of that measured for the specimens loaded with an axial stress of $0.7 f'_c$.

(5) The shear stress versus shear displacement behavior of the specimens cycled in shear under constant crack widths resulted in strength and stiffness degrading pinched hysteretic loops.

6.1.3 Behavior of Barbell-Shaped Isolated Shear Walls

(1) The high shear strength and stiffness of edge members under axial compression limits the likelihood of sliding shear failure in

barbell-shaped walls. Web crushing must first occur to sufficiently increase the height of the sliding region in the panel, only then will short column behavior of the edge members be induced.

(2) Tension in an edge member producing yielding of the longitudinal steel and wide cracking of the concrete will reduce the overall shear strength and stiffness of the wall as it is cycled in shear. If cracks are not closed by compression yielding of the steel, only the reinforcement in the edge members will be capable of resisting lateral loads.

6.2 Recommendations for Future Research

Results of the reported investigation suggest modifications and/or further studies in the following areas.

6.2.1 Testing Facility

(1) To enable the study of specimens subjected to axial stresses in excess of $0.7 f'_c$ and/or those longitudinally reinforced, the testing facility should be modified to accommodate the increased shear force demand. Alternatively, the specimen test section could be decreased in size to reduce the demand.

(2) To assure accurate measurement of the shear force resisted by a specimen, the frictional losses in the test frame should be monitored. A load cell placed on the opposite side of the specimen from the shear loading jack may be found suitable.

(3) An improved scheme to resist rotation of the bottom half of the specimen is advisable. Screw jacks were used to block the pinned connection beneath the specimen for a temporary rotational restraint.

6.2.2 Test Specimen

(1) The reasons for the low experimental shear moduli should be investigated further.

(2) The core height should be increased to study the effect of confinement on the shear strength and stiffness of edge members as well as to investigate the conditions under which diagonal tension failure occurs in edge members. The introduction of bending will permit a more in depth study of dowel action or short column behavior.

(3) Longitudinal steel should be added to the specimens to study the relative contributions of concrete and steel to the shear strength and stiffness of edge members. This will permit an assessment of their interaction and an understanding of the overall behavior of edge members.

(4) Under extreme seismic excitations, edge members will likely be subjected to axial loads in excess of those applied to the specimens reported on in this investigation ($0.7 f'_c$). Axial loads close to the compressive strength of the specimens should be applied to provide data over the entire range of potential compressive forces.

Longitudinally reinforced specimens should also be subjected to axial loads large enough to cause tensile yielding of the steel and wide cracking in the concrete.

(5) Additional tests should be performed with a range of crack widths maintained constant during shear loading.

Once the testing procedure is refined and the basic behavior of edge members is understood the effects of several additional parameters should be studied. These include the amount and type of confinement, load history, rate of loading, concrete strength, and aggregate type.

REFERENCES

1. Bertero, V. V., "Seismic Performance of Reinforced Concrete Structures," Anales de la Academia Nacional de Ciencias Exactas. Fisicas y Naturales, Buenos Aires, 1979, Tomo 31, pp. 113-138.
2. Sharpe, R. L., "The Earthquake Problem," ACI Publication SP-53, Detroit, Michigan, 1977, pp. 25-35.
3. Park, R., and Paulay, T., Reinforced Concrete Structures. John Wiley and Sons, New York, 1975.
4. Wang, T. Y., Bertero, V. V., and Popov, E. P., "Hysteretic Behavior of Reinforced Concrete Framed Walls," Report No. EERC 75-23, Earthquake Engineering Research Center, University of California, Berkeley, December 1975.
5. Vallenias, J. M., Bertero, V. V., and Popov, E. P., "Hysteretic Behavior of Reinforced Concrete Structural Walls," Report No. EERC-79/20, Earthquake Engineering Research Center, University of California, Berkeley, August 1979.
6. Iliya, R. and Bertero, V. V., "Effects of Amount and Arrangement of Wall-Panel Reinforcement on Hysteretic Behavior of Reinforced Concrete Walls," Report No. EERC 80/04, Earthquake Engineering Research Center, University of California, Berkeley, February 1980.
7. Oesterle, R. G. et al., "Earthquake Resistant Structural Walls - Tests of Isolated Walls - Phase II," PCA R/D Ser. 1629, Construction Technology Laboratories, Skokie, Illinois, October 1979.
8. Aktan, A. E. and Bertero, V. V., "The Seismic Resistant Design of R/C Coupled Structural Walls," Report No. EERC 81-07, Earthquake Engineering Research Center, University of California, Berkeley, June 1981.
9. Building Code Requirements for Reinforced Concrete (ACI, 318-77), American Concrete Institute, Detroit, Michigan, 1977.
10. Urquhart, L., O'Rourke, C., and Winter, G., DESIGN OF CONCRETE STRUCTURES, McGraw-Hill Book Company, Inc., 1958, p. 27.
11. Bresler, B. and Pister, K. S., "Strength of Concrete Under Combined Stresses," Proceedings, American Concrete Institute, Detroit, Michigan, Vol. 55, September 1958, pp. 321-345.
12. Taylor, M. A. and Broms, B. B., "Shear Bond Strength Between Coarse Aggregate and Cement Paste or Mortar," Journal, American Concrete Institute, Detroit, Michigan, Vol. 61, No. 8, August 1964, pp. 939-956.
13. Jimenez-Perez, R., Gergely, P., and White, R. N., "Shear Transfer Across Cracks in Reinforced Concrete," Report 78-4, Cornell University, Ithaca, New York, August 1978.

TABLES

TABLE 2.1 - CONCRETE MIX

Material	Wt. for 1 cu. yd.* (lbs)**
Cement Type I	636
Fine Sand	325
Coarse Sand	1316
Aggregate	1287
Water	326

* 1 cu. yd. = 0.765 m³

** 1 lb. = 4.45 N

TABLE 2.2 MECHANICAL CHARACTERISTICS OF CONCRETE

Specimen	Age (days)	Avg. Cylinder Strength, f'_c (psi)*	Splitting Tensile Stress (psi)	Modulus of Rupture, f_r (psi)	Tangent Modulus of Elasticity (ksi)**	Secant Modulus of Elasticity, E_c (ksi)	E_c per ACI Eqn. (ksi)	ϵ_0
S1U1	48	5140	419	534	-	-	4087	-
S1U2	64	5155	456	696	-	-	4093	-
S1U3	53	5146	453	617	2700	2625	4089	0.0028
S1U4	60	5164	506	662	-	-	4096	-
S1C1	60	5278	428	595	-	-	4141	-
S1C2	69	5200	498	745	3300	3050	4110	0.0030
S1C3	56	5330	506	586	2930	2768	4161	0.0036
S1C4	64	5022	566	663	2900	2649	4039	0.0023

* 1 psi = 6895 Pa

** 1 ksi = 6.895 MPa

TABLE 3.1 - AXIAL LOADS APPLIED DURING TESTING

Specimen	Axial Stress During Monotonic Shear Loading	Axial Stress During Shear Cycling	Constant Average Crack Width During Cycling
S1U1	0	-	-
S1U2	0.45 f'_c	0.45 f'_c	-
S1U3	0.7 f'_c	0.7 f'_c	-
S1U4	-	-	0.05" (1 cycle)
S1C1	-	0.16 f'_c	-
S1C2	0.45 f'_c	0.45 f'_c	-
S1C3	0.7 f'_c	0.7 f'_c	-
S1C4(a)	-0.2 f'_c	-	0.02"
(b)	-	0.3 f'_c	-

(- not included in test)

Specimen Designation

1 in. = 25.4 mm

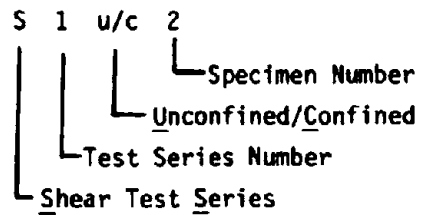



TABLE 4.1 - COMPARISON OF EXPERIMENTAL AND THEORETICAL SHEAR MODULI

Specimen	Axial Stress, p	Experimental Shear Modulus, G (ksi)*	Average Theoretical Shear Modulus, G (ksi)
S1C4	$-0.2 f'_c$	300	1200 
S1U1	0	310	
S1U2	$0.45 f'_c$	330	
S1C2	$0.45 f'_c$	280	
S1U3	$0.7 f'_c$	560	
S1C3	$0.7 f'_c$	540	

* 1 ksi = 6.895 MPa

TABLE 4.2 - COMPARISON OF EXPERIMENTAL AND THEORETICAL SHEAR STRENGTHS OF INITIALLY UNCRACKED SPECIMENS

Specimen	Axial Stress p (psi)	Shear Strength, v_u (psi)*		
		Experimental	Analytical	
			(1)	(2)
S1C4	-94	318	0	346
S1U1	0	366	143	406
S1U2	2177	2516	300	813
S1C2	2200	2617	303	987
S1U3	3513	3116	395	754
S1C3	3536	3339	404	1234

* 1 psi = 6895 Pa

$$(1) \quad V_c = 2 \left(1 + \frac{N_u}{2000 A_g} \right) \sqrt{f'_c} \quad b_w d \quad [\text{Ref. 9}]$$

$$v_u = V_c / A_g$$

$$(2) \quad \tau_a = 0.949 \sigma_a + 0.05 f'_c \quad [\text{Ref. 11}]$$

$$\text{where } \tau_a = \sqrt{\frac{2}{15}} [I_1^2 - 3I_2]^{\frac{1}{2}}$$

$$\sigma_a = \frac{1}{3} I_1$$

FIGURES

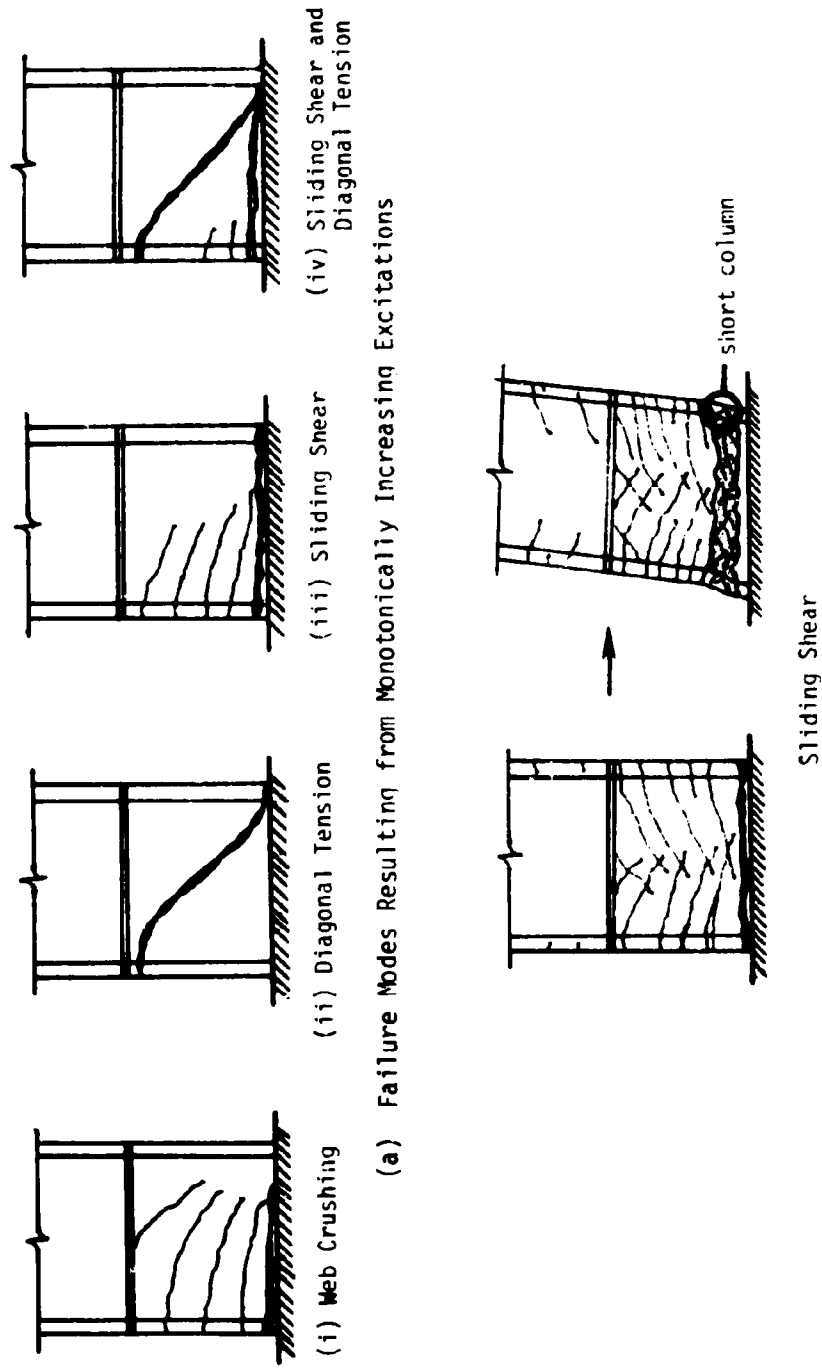


Fig. 1.1 Shear Wall Failure Modes

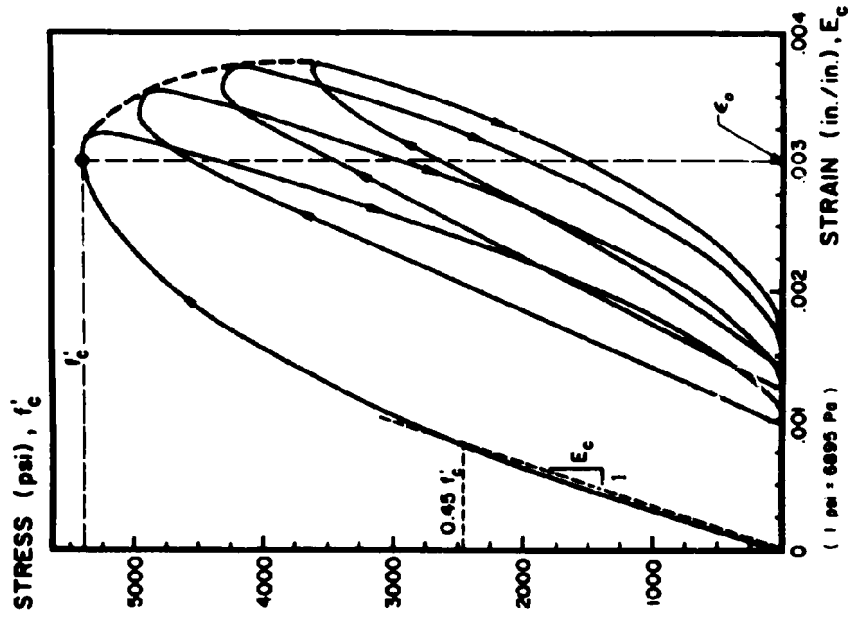


Fig. 2.2 Concrete Stress-Strain Diagram

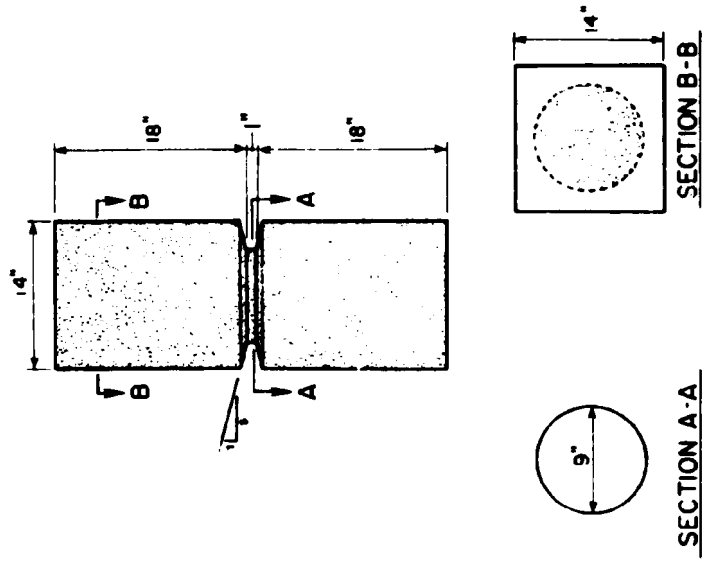


Fig. 2.1 Test Specimen Geometry

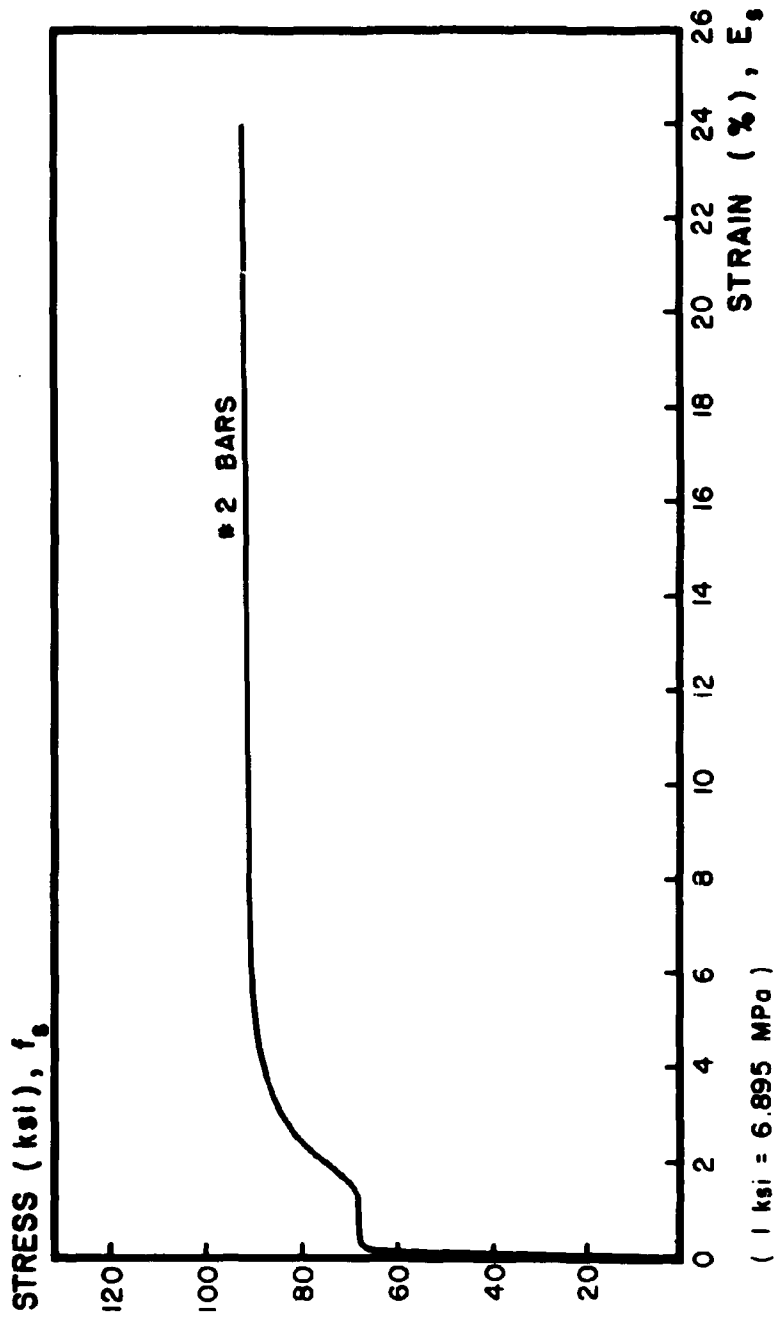
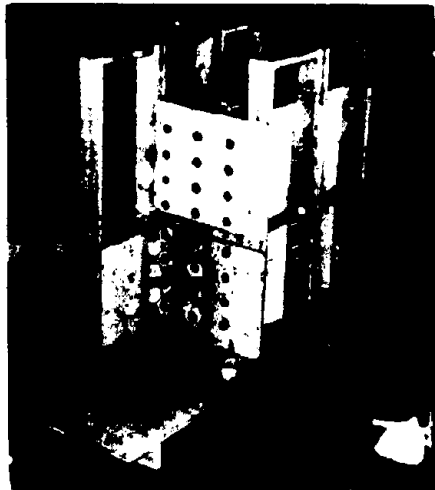
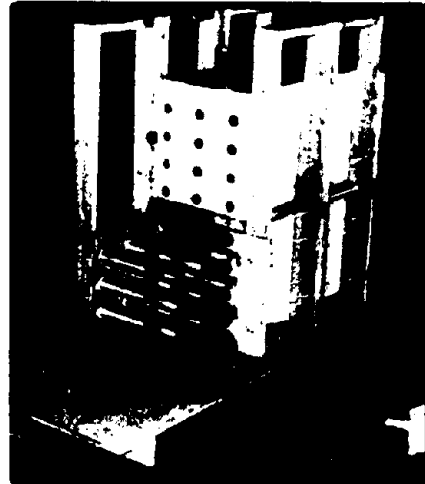


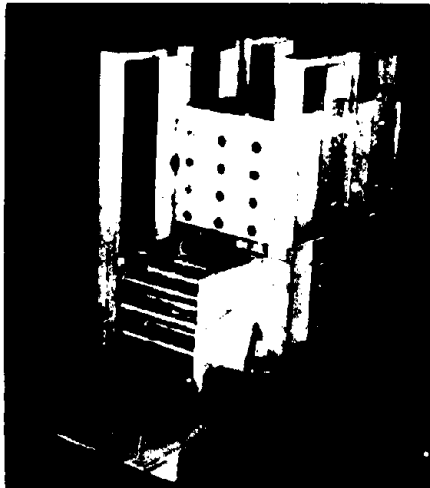
Fig. 2.3 Stress-Strain Relationship of the #2 Reinforcing Bar Used for the Spiral



(a)



(b)

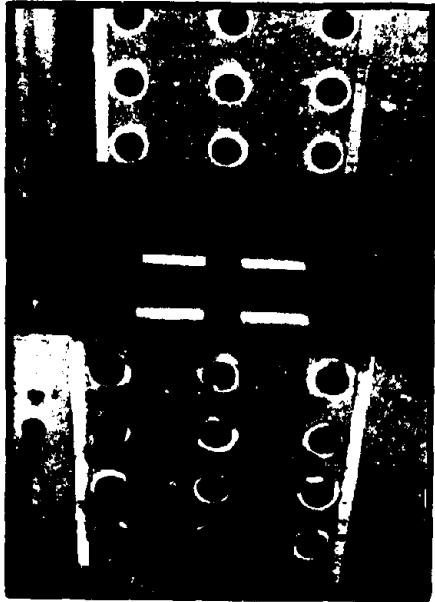


(c)

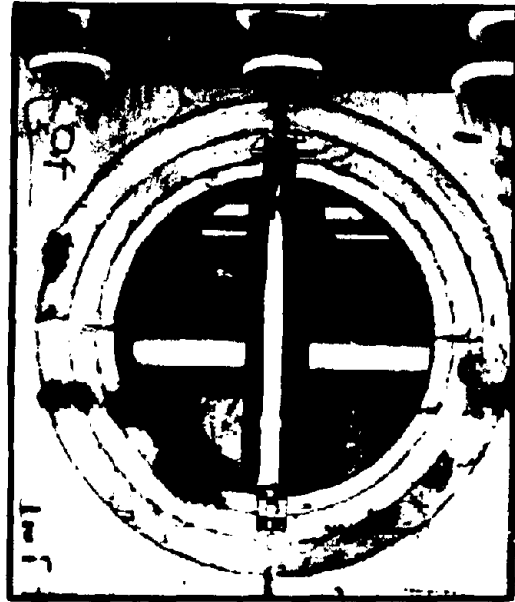


(d)

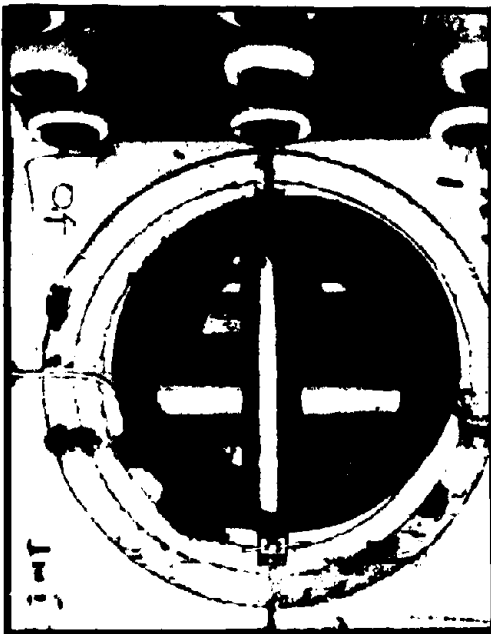
Fig. 2.4 Formwork Assemblage Procedure



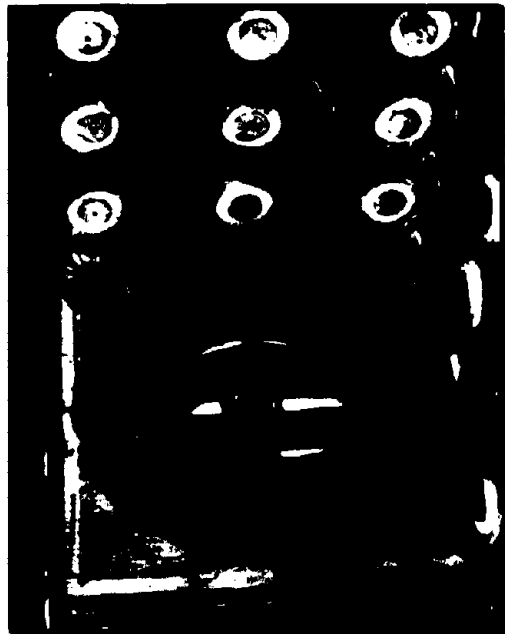
(e)



(f)



(g)



(h)

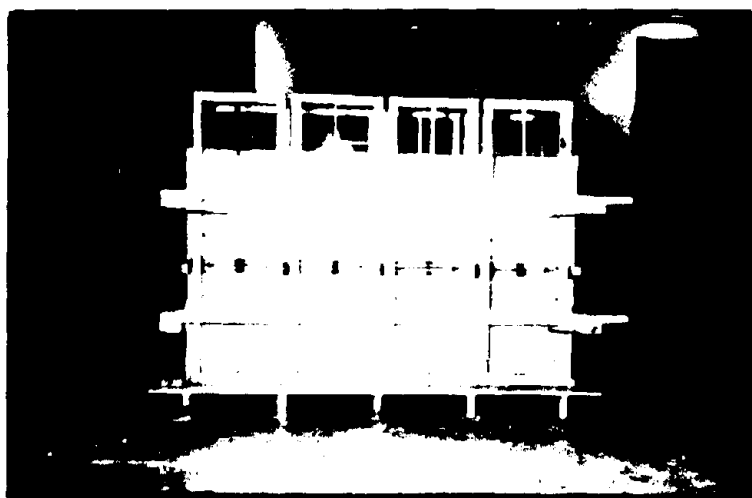
Fig. 2.4 Continued
51



(i)



(j)



(k)

Fig. 2.4 Continued

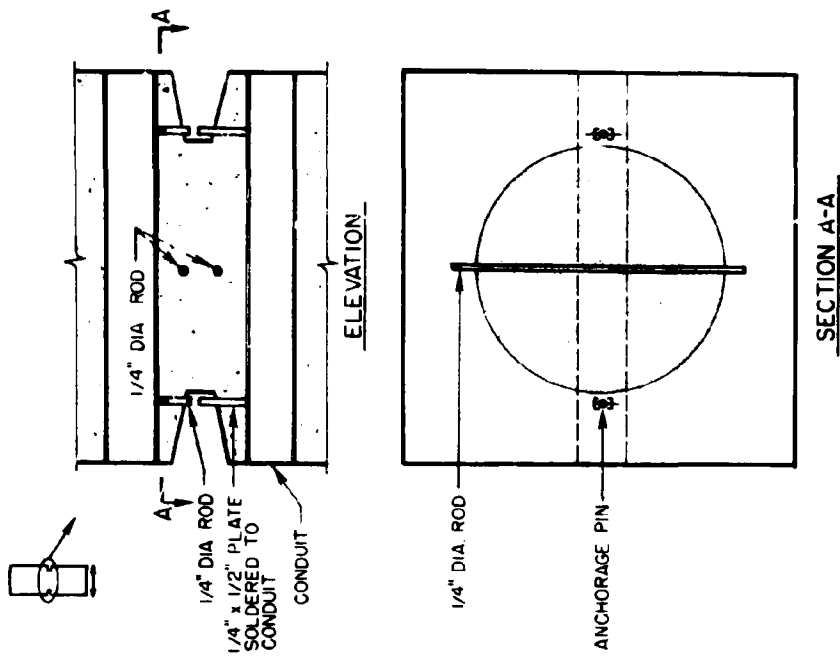


Fig. 2.6 Placement of Instrumentation Fixtures

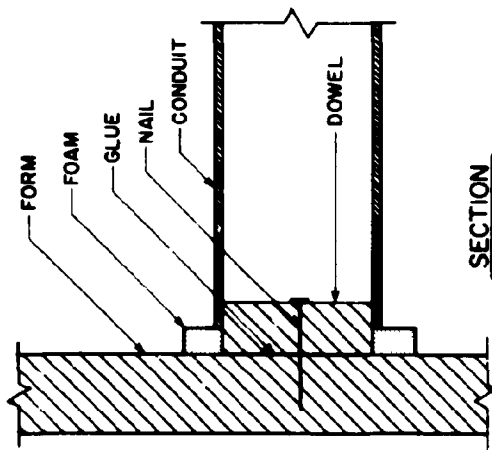


Fig. 2.5 Conduit Support Detail

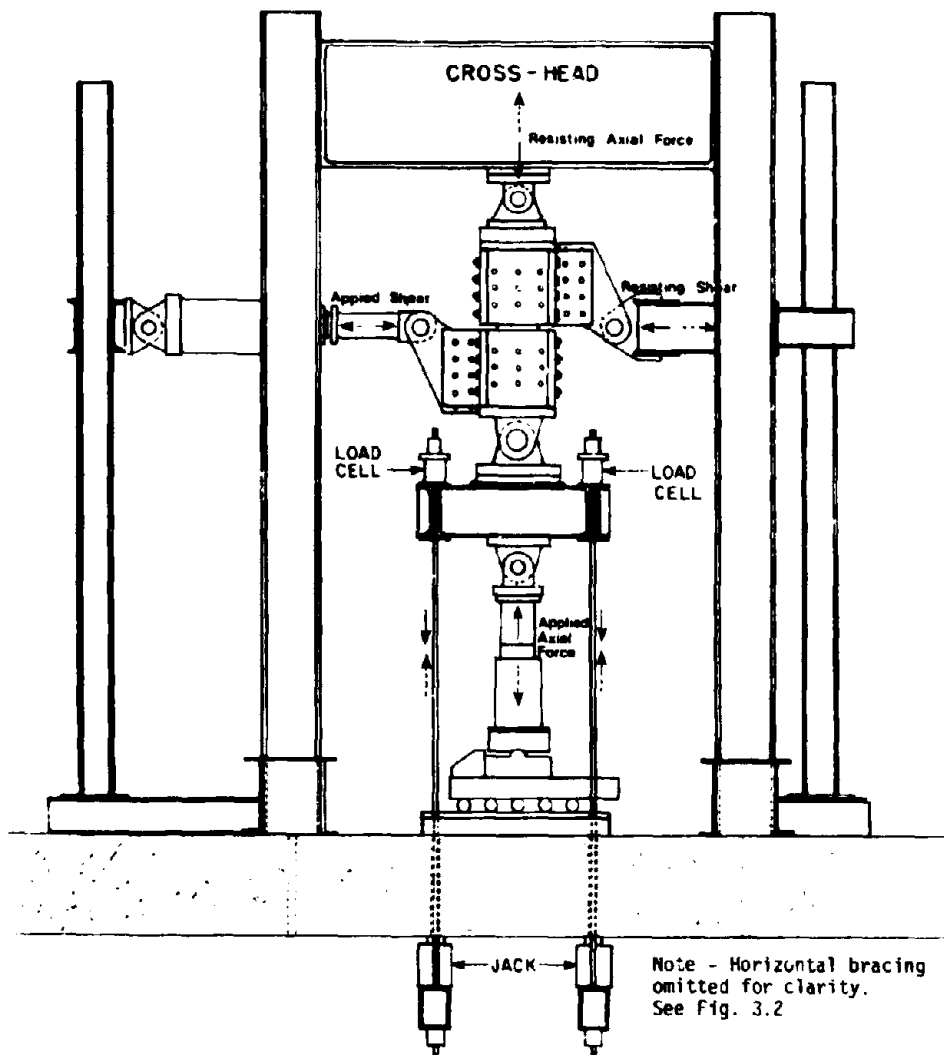


Fig. 3.1 Experimental Setup

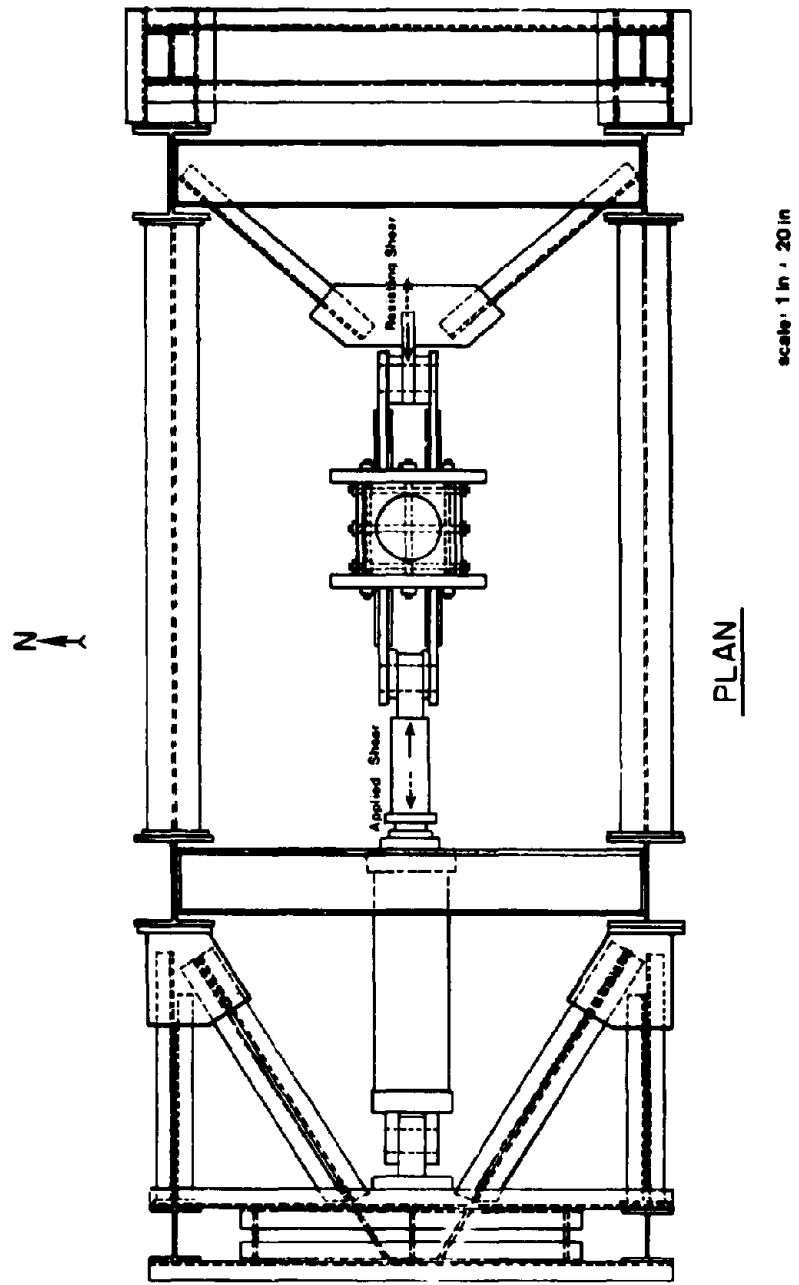


Fig. 3.2 Shear Reaction Bracing

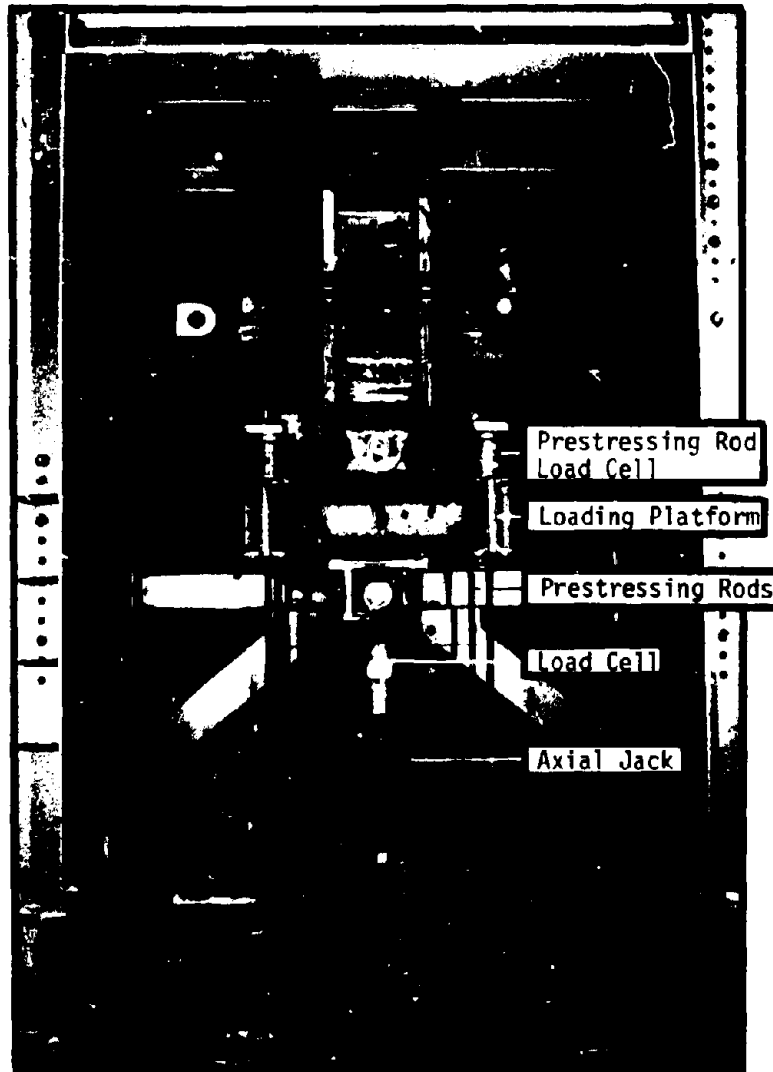


Fig. 3.3 Axial Loading System

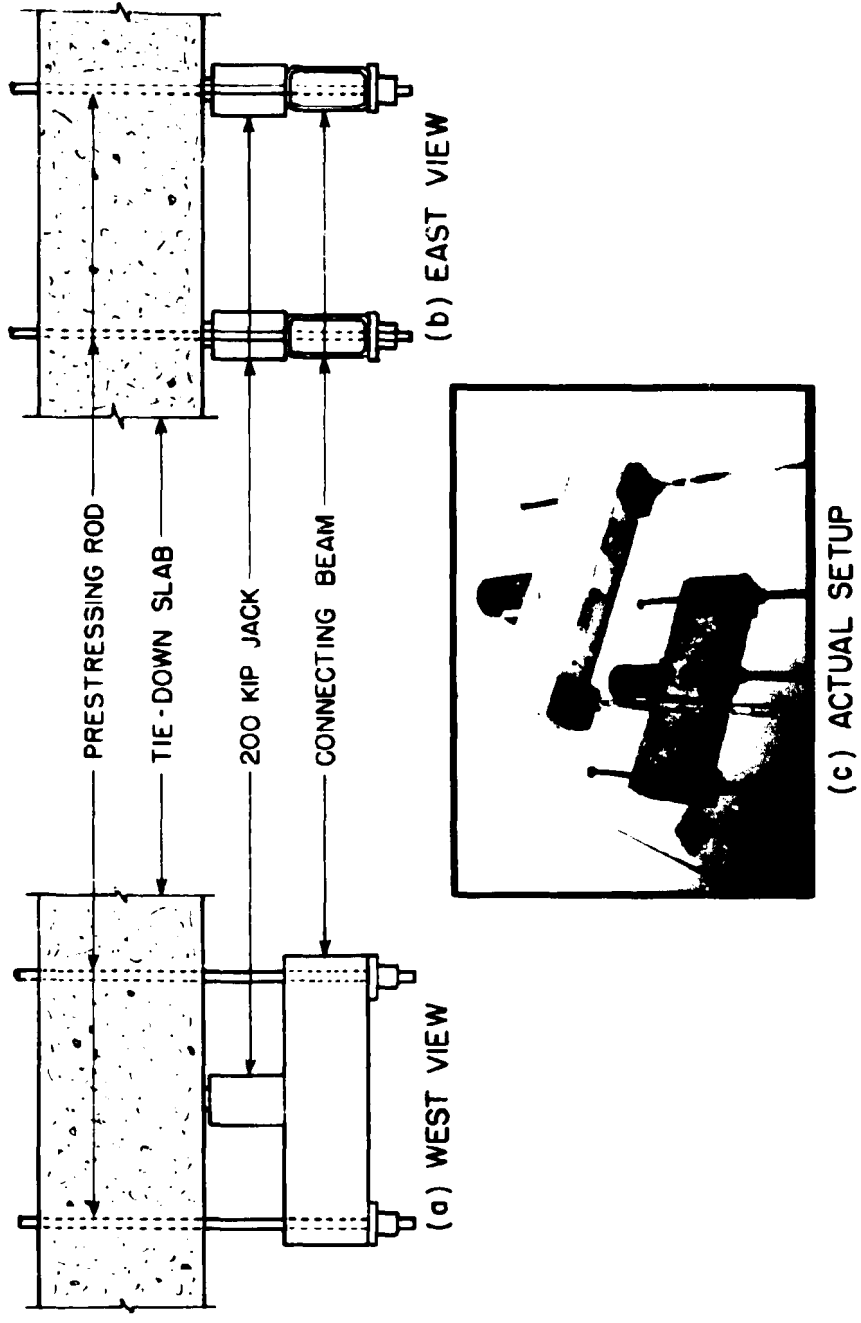


Fig. 3.4 Axial Loading Apparatus

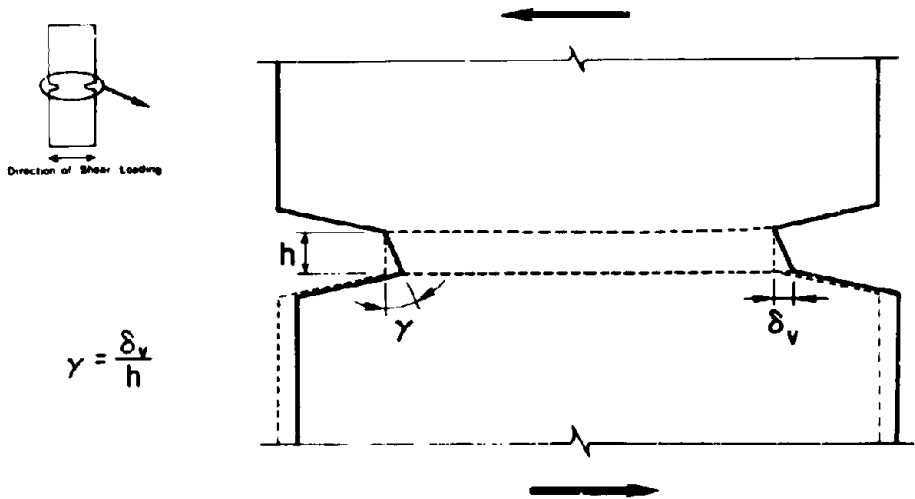
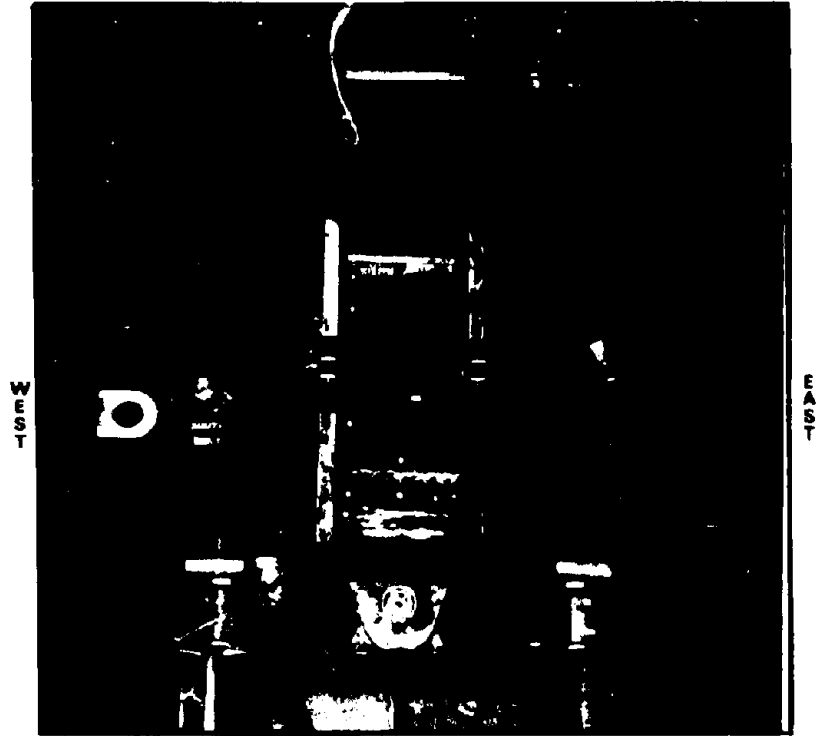


Fig. 3.6 Specimen Shear Deformations

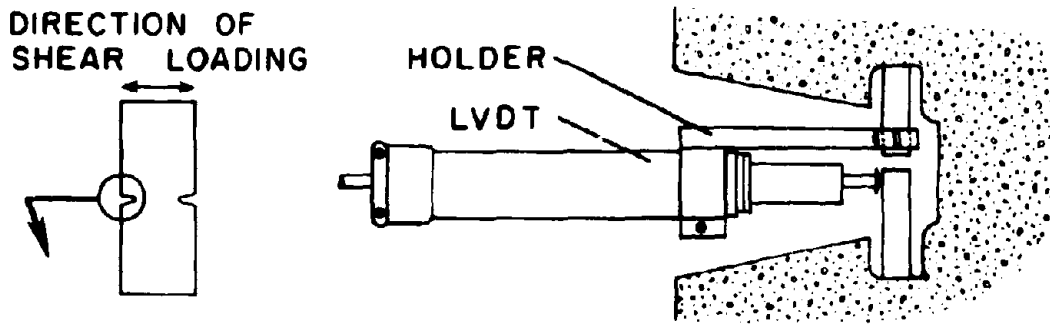


Fig. 3.7 Shear Deformation Instrumentation - Scheme 1

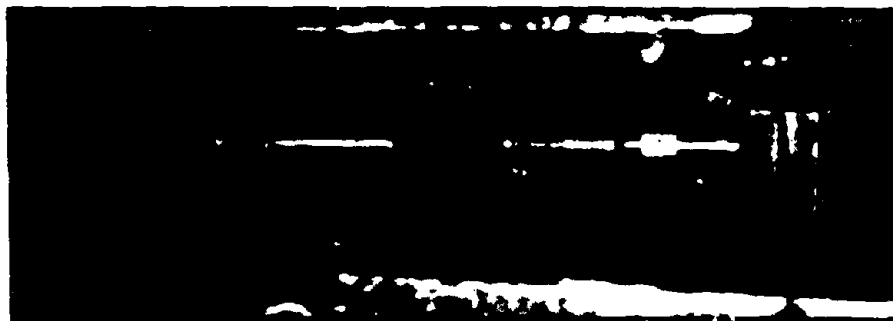
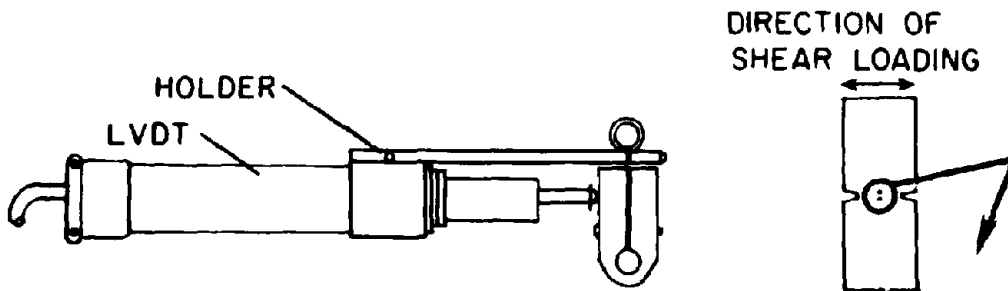


Fig. 3.8 Shear Deformation Instrumentation - Scheme 2

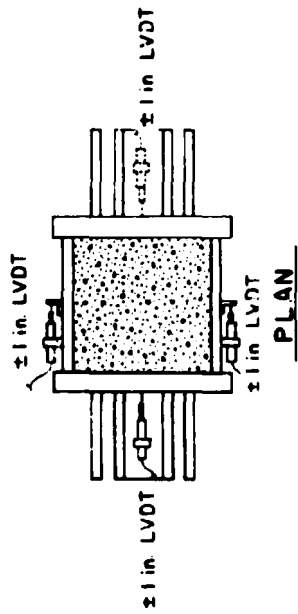


Fig. 3.9 Placement of Shear Displacement Instrumentation Mounted on Steel Plates

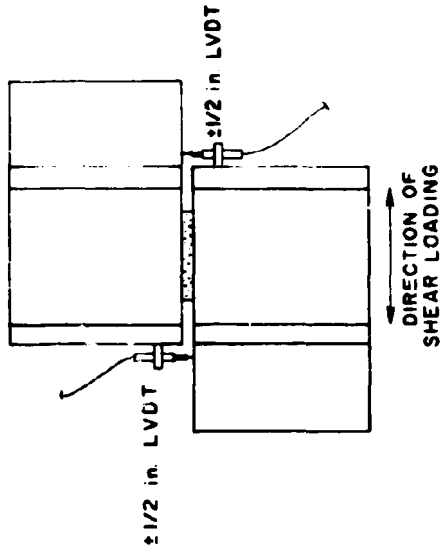


Fig. 3.10 Placement of Axial Deformation Instrumentation

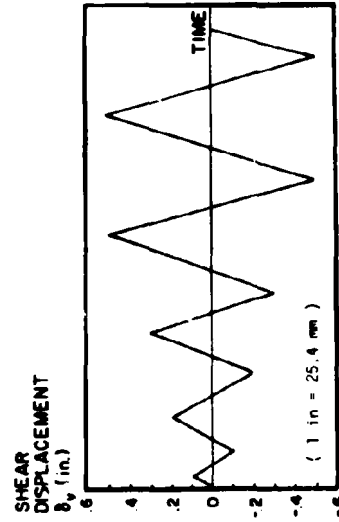
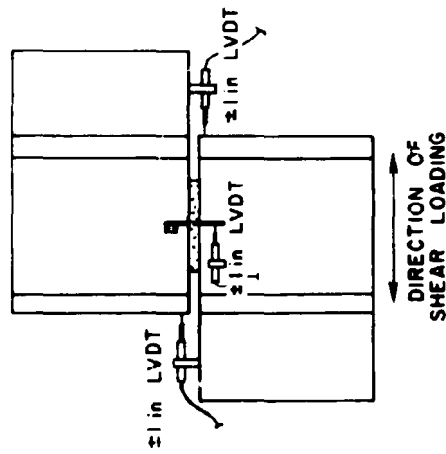


Fig. 3.11 Typical Loading Program



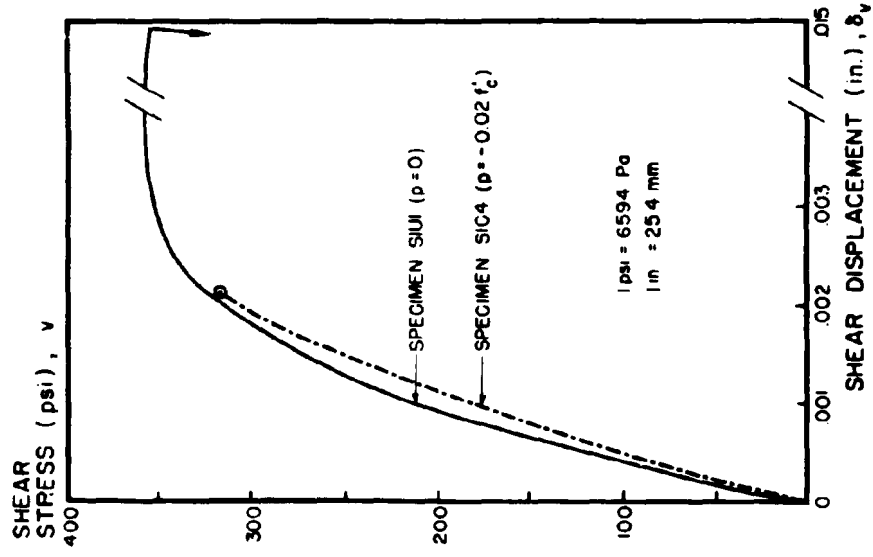


Fig. 4.2 Comparison of Monotonic $v-\delta_v$ Diagrams, Specimens SIC1 and SIC4

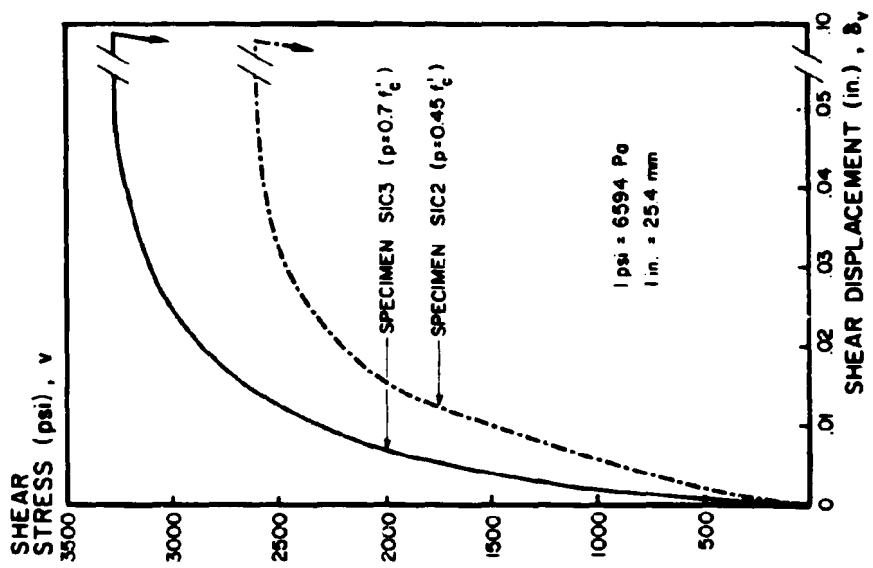


Fig. 4.1 Comparison of Monotonic $v-\delta_v$ Diagrams, Specimens SIC2 and SIC3

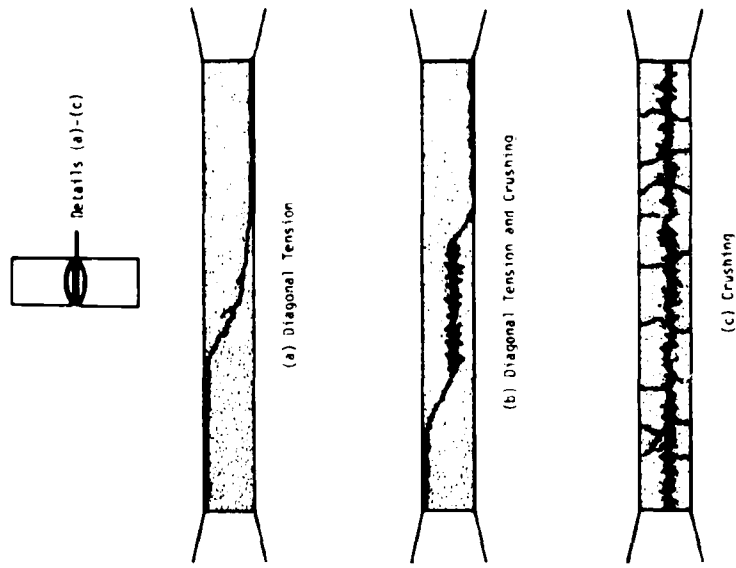


Fig. 4.4 Observed Failure Modes

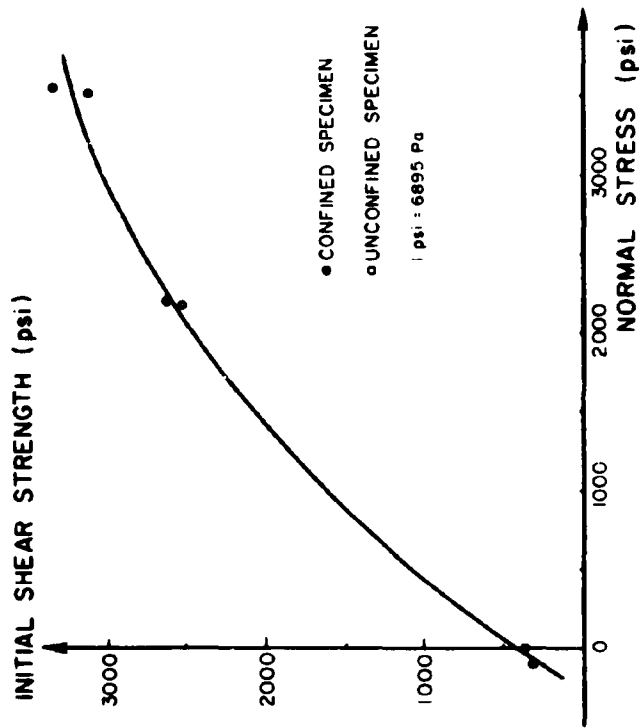


Fig. 4.3 Relationship of Initial Shear Strength to Normal Stress

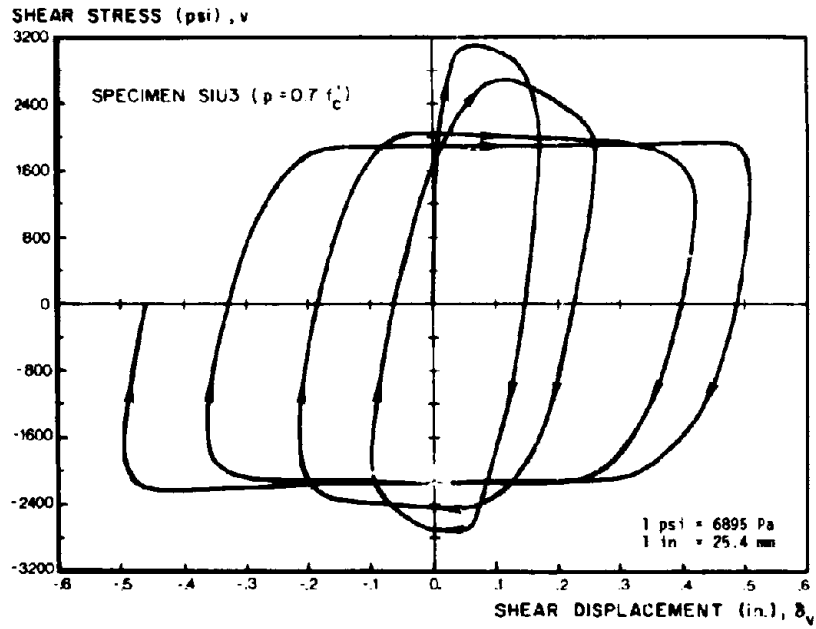


Fig. 4.5 Typical Cyclic v - δ_v Diagram

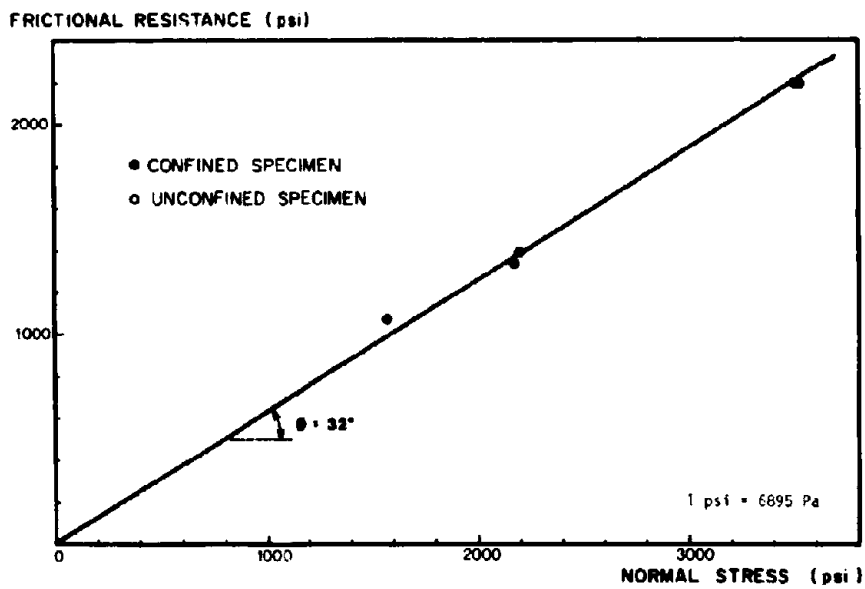


Fig. 4.6 Frictional Shear Resistance Versus Normal Stress Diagram

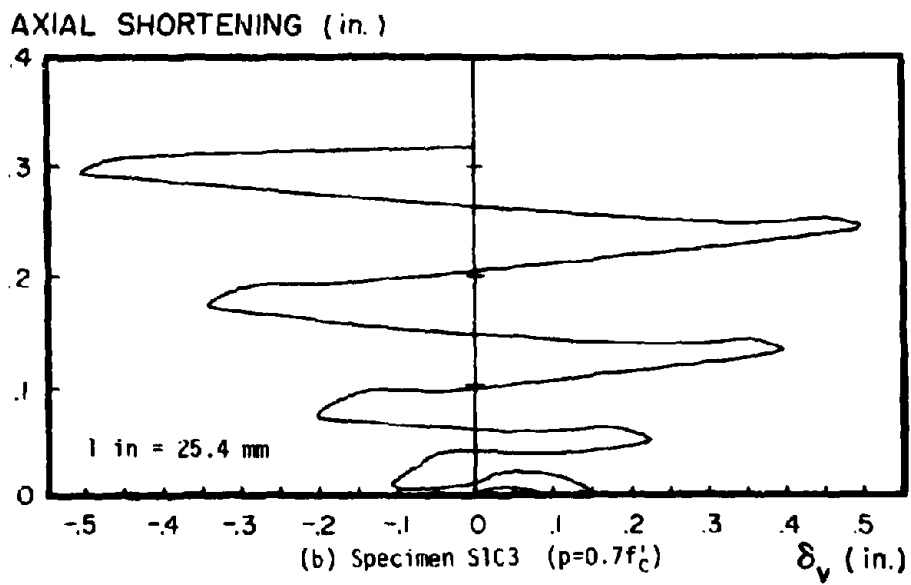
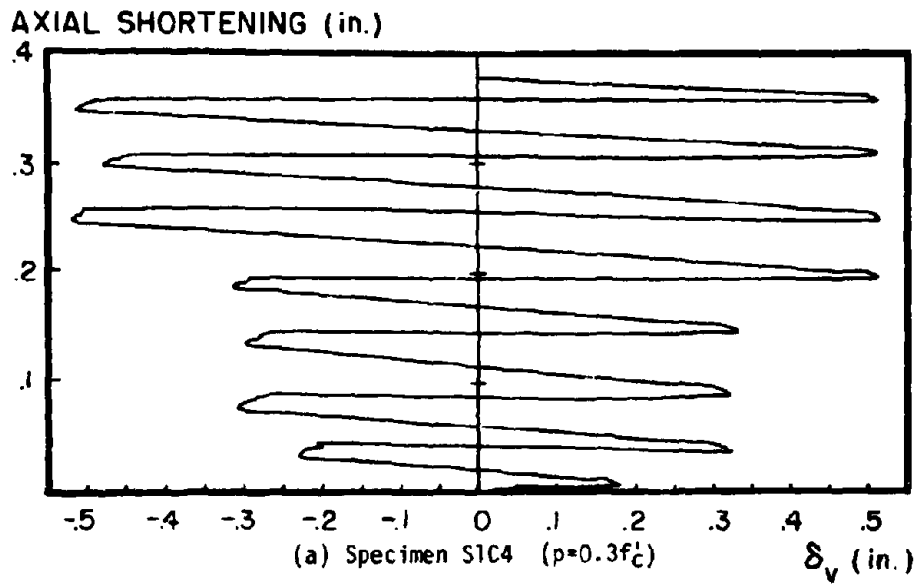
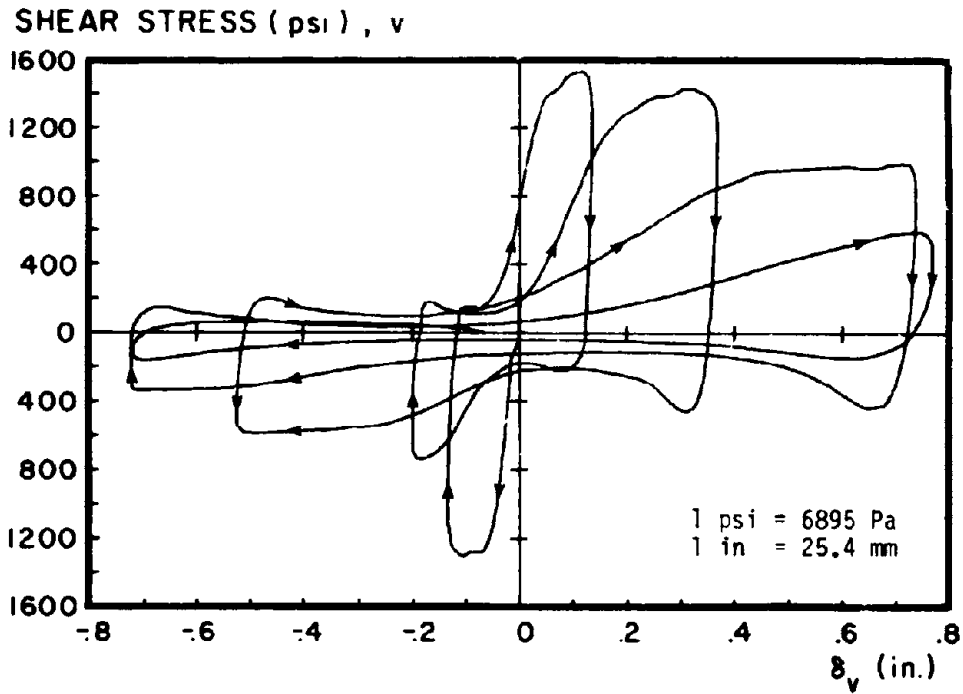
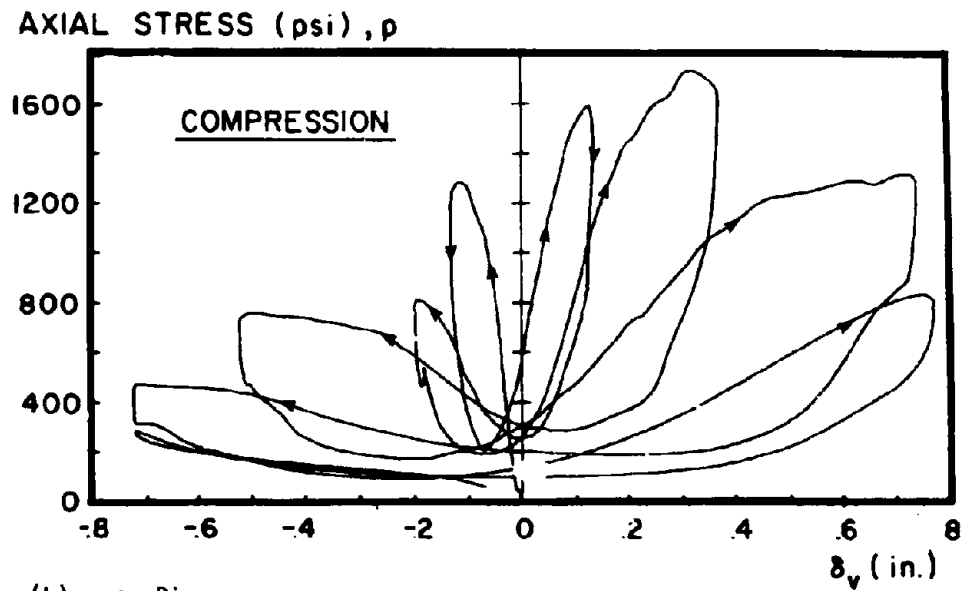


Fig. 4.7 Axial Shortening Versus Shear Displacement Diagrams, Specimens S1C3 and S1C4



(a) v - δ_v Diagrams



(b) p - δ_v Diagrams

Fig. 4.8 v - δ_v and p - δ_v Diagrams for Specimen S1C4
Cycled under a Constant Average Crack Width of 0.02 in.

EARTHQUAKE ENGINEERING RESEARCH CENTER REPORTS

NOTE: Numbers in parentheses are Accession Numbers assigned by the National Technical Information Service; these are followed by a price code. Copies of the reports may be ordered from the National Technical Information Service, 5285 Port Royal Road, Springfield, Virginia, 22161. Accession Numbers should be quoted on orders for reports (PB --- ---) and remittance must accompany each order. Reports without this information were not available at time of printing. The complete list of EERC reports (from EERC 67-1) is available upon request from the Earthquake Engineering Research Center, University of California, Berkeley, 47th Street and Hoffman Boulevard, Richmond, California 94804.

- UCB/EERC-77/01 "PLUSH - A Computer Program for Probabilistic Finite Element Analysis of Seismic Soil-Structure Interaction," by M.F. Romo Organista, J. Lysmer and H.B. Seed - 1977 (PB81 177 651)A05
- UCB/EERC-77/02 "Soil-Structure Interaction Effects at the Humboldt Bay Power Plant in the Ferndale Earthquake of June 7, 1975," by J.E. Valera, H.B. Seed, C.C. Tsai and J. Lysmer - 1977 (PB 265 795)A04
- UCB/EERC-77/03 "Influence of Sample Disturbance on Sand Response to Cyclic Loading," by K. Mori, H.B. Seed and C.K. Chan - 1977 (PB 267 352)A04
- UCB/EERC-77/04 "Seismological Studies of Strong Motion Records," by J. Shoja-Taheri - 1977 (PB 269 655)A10
- UCB/EERC-77/05 Unassigned
- UCB/EERC-77/06 "Developing Methodologies for Evaluating the Earthquake Safety of Existing Buildings," by No. 1 - B. Bresler; No. 2 - B. Bresler, T. Okada and D. Zisling; No. 3 - T. Okada and B. Bresler; No. 4 - V.V. Bertero and B. Bresler - 1977 (PB 267 354)A08
- UCB/EERC-77/07 "A Literature Survey - Transverse Strength of Masonry Walls," by Y. Omote, R.L. Mayes, S.W. Chen and R.W. Clough - 1977 (PB 277 333)A07
- UCB/EERC-77/08 "DRAIN-TABS: A Computer Program for Inelastic Earthquake Response of Three Dimensional Buildings," by R. Guendelman-Israel and G.H. Powell - 1977 (PB 270 693)A07
- UCB/EERC-77/09 "SUBWALL: A Special Purpose Finite Element Computer Program for Practical Elastic Analysis and Design of Structural Walls with Substructure Option," by D.C. Le, M. Peterson and E.P. Popov - 1977 (PB 270 567)A05
- UCB/EERC-77/10 "Experimental Evaluation of Seismic Design Methods for Broad Cylindrical Tanks," by D.P. Clough (PB 272 280)A13
- UCB/EERC-77/11 "Earthquake Engineering Research at Berkeley - 1976," - 1977 (PB 273 507)A09
- UCB/EERC-77/12 "Automated Design of Earthquake Resistant Multistory Steel Building Frames," by N.D. Walker, Jr. - 1977 (PB 276 526)A09
- UCB/EERC-77/13 "Concrete Confined by Rectangular Hoops Subjected to Axial Loads," by J. Vallenias, V.V. Bertero and E.P. Popov - 1977 (PB 275 165)A06
- UCB/EERC-77/14 "Seismic Strain Induced in the Ground During Earthquakes," by Y. Sugimura - 1977 (PB 284 201)A04
- UCB/EERC-77/15 Unassigned
- UCB/EERC-77 16 "Computer Aided Optimum Design of Ductile Reinforced Concrete Moment Resisting Frames," by S.W. Zaczajski and V.V. Bertero - 1977 (PB 280 137)A07
- UCB/EERC-77/17 "Earthquake Simulation Testing of a Stepping Frame with Energy-Absorbing Devices," by J.M. Kelly and D.F. Tsztsoo - 1977 (PB 273 506)A04
- UCB/EERC-77/18 "Inelastic Behavior of Eccentrically Braced Steel Frames under Cyclic Loadings," by C.W. Roeder and E.P. Popov - 1977 (PB 275 526)A15
- UCB/EERC-77/19 "A Simplified Procedure for Estimating Earthquake-Induced Deformations in Dams and Embankments," by F.I. Makdisi and H.B. Seed - 1977 (PB 276 820)A04
- UCB/EERC-77/20 "The Performance of Earth Dams during Earthquakes," by H.B. Seed, F.I. Makdisi and P. de Alba - 1977 (PB 276 821)A04
- UCB/EERC-77/21 "Dynamic Plastic Analysis Using Stress Resultant Finite Element Formulation," by P. Lukkunaprasit and J.M. Kelly - 1977 (PB 275 453)A04
- UCB/EERC-77/22 "Preliminary Experimental Study of Seismic Uplift of a Steel Frame," by R.W. Clough and A.A. Huckelbridge 1977 (PB 278 769)A08
- UCB/EERC-77/23 "Earthquake Simulator Tests of a Nine-Story Steel Frame with Columns Allowed to Uplift," by A.A. Huckelbridge - 1977 (PB 277 944)A09
- UCB/EERC-77/24 "Nonlinear Soil-Structure Interaction of Skew Highway Bridges," by M.-C. Chen and J. Penzien - 1977 (PB 276 176)A07
- UCB/EERC-77/25 "Seismic Analysis of an Offshore Structure Supported on Pile Foundations," by D.D.-N. Liou and J. Penzien 1977 (PB 283 180)A06
- UCB/EERC-77/26 "Dynamic Stiffness Matrices for Homogeneous Viscoelastic Half-Planes," by G. Dargupta and A.K. Chopra - 1977 (PB 279 654)A06

UCB/EERC-77/27 "A Practical Soft Story Earthquake Isolation System," by J.M. Kelly, J.M. Eidinger and C.J. Derham - 1977 (PB 276 814)A07

UCB/EERC-77/29 "Seismic Safety of Existing Buildings and Incentives for Hazard Mitigation in San Francisco: An Exploratory Study," by A.J. Meltaner - 1977 (PB 281 970)A05

UCB/EERC-77/29 "Dynamic Analysis of Electrohydraulic Shaking Tables," by D. Isea, S. Abedi-Mayati and Y. Takanashi 1977 (PB 282 569)A04

UCB/EERC-77/30 "An Approach for Improving Seismic - Resistant Behavior of Reinforced Concrete Interior Joints," by B. Galuric, V.V. Bertero and E.P. Popov - 1977 (PB 290 870)A06

UCB/EERC-78/01 "The Development of Energy-Absorbing Devices for Seismic Base Isolation Systems," by J.M. Kelly and D.F. Tsitoo - 1978 (PB 284 978)A04

UCB/EERC-78/02 "Effect of Tensile Prestrain on the Cyclic Response of Structural Steel Connections," by J.G. Bouwkamp and A. Mukhopadhyay - 1978

UCB/EERC-78/03 "Experimental Results of an Earthquake Isolation System using Natural Rubber Bearings," by J.M. Eidinger and J.M. Kelly - 1978 (PB 281 686)A04

UCB/EERC-78/04 "Seismic Behavior of Tall Liquid Storage Tanks," by A. Niwa - 1978 (PB 284 017)A14

UCB/EERC-78/05 "Hysteretic Behavior of Reinforced Concrete Columns Subjected to High Axial and Cyclic Shear Forces," by S.W. Zagajewski, V.V. Bertero and J.G. Bouwkamp - 1978 (PB 283 858)A13

UCB/EERC-78/06 "Three Dimensional Inelastic Frame Elements for the ANSR-2 Program," by A. Riahi, D.G. Row and J.H. Powell - 1978 (PB 295 755)A04

UCB/EERC-78/07 "Studies of Structural Response to Earthquake Ground Motion," by O.A. Lopez and A.K. Chopra - 1978 (PB 282 790)A05

UCB/EERC-78/08 "A Laboratory Study of the Fluid-Structure Interaction of Submerged Tanks and Caissons in Earthquakes," by R.C. Byrd - 1978 (PB 284 957)A08

UCB/EERC-78/09 Unassigned

UCB/EERC-78/10 "Seismic Performance of Nonstructural and Secondary Structural Elements," by I. Sakamoto - 1978 (PB81 154 593)A05

UCB/EERC-78/11 "Mathematical Modelling of Hysteresis Loops for Reinforced Concrete Columns," by S. Nakata, T. Sproul and J. Penzien - 1978 (PB 298 274)A05

UCB/EERC-78/12 "Damageability in Existing Buildings," by T. Szejwas and B. Bresler - 1978 (PB 80 166 978)A05

UCB/EERC-78/13 "Dynamic Behavior of a Pedestal Base Multistory Building," by R.M. Stephen, E.L. Wilson, J.G. Bouwkamp and M. Butten - 1978 (PB 286 650)A08

UCB/EERC-78/14 "Seismic Response of Bridges - Case Studies," by R.A. Imbsen, V. Nutt and J. Penzien - 1978 (PB 286 503)A10

UCB/EERC-78/15 "A Substructure Technique for Nonlinear Static and Dynamic Analysis," by D.T. Row and G.H. Powell - 1978 (PB 288 077)A10

UCB/EERC-78/16 "Seismic Risk Studies for San Francisco and for the Greater San Francisco Bay Area," by C.S. Oliveira - 1978 (PB 81 120 115)A07

UCB/EERC-78/17 "Strength of Timber Roof Connections Subjected to Cyclic Loads," by P. Gülkan, R.L. Mayes and R.W. Clough - 1978 (HUD-000 1491)A07

UCB/EERC-78/18 "Response of K-Braced Steel Frame Models to Lateral Loads," by J.G. Bouwkamp, R.M. Stephen and E.P. Popov - 1978

UCB/EERC-78/19 "Rational Design Methods for Light Equipment in Structures Subjected to Ground Motion," by J.L. Sackman and J.M. Kelly - 1978 (PB 292 357)A04

UCB/EERC-78/20 "Testing of a Wind Restraint for Seismic Base Isolation," by J.M. Kelly and D.E. Chitty - 1978 (PB 292 833)A03

UCB/EERC-78/21 "APOLLO - A Computer Program for the Analysis of Pore Pressure Generation and Dissipation in Horizontal Sand Layers During Cyclic or Earthquake Loading," by P.P. Martin and H.B. Seed - 1978 (PB 292 835)A04

UCB/EERC-78/22 "Optimal Design of an Earthquake Isolation System," by M.A. Bhatti, K.S. Pister and E. Polak - 1978 (PB 294 735)A06

UCB/EERC-78/23 "NASH - A Computer Program for the Non-Linear Analysis of Vertically Propagating Shear Waves in Horizontally Layered Deposits," by P.P. Martin and H.B. Seed - 1978 (PB 293 101)A05

UCB/EERC-78/24 "Investigation of the Elastic Characteristics of a Three Story Steel Frame Using System Identification," by I. Kaya and H.D. McIven - 1978 (PB 296 225)A06

UCB/EERC-78/25 "Investigation of the Nonlinear Characteristics of a Three-Story Steel Frame Using System Identification," by I. Kaya and H.D. McIven - 1978 (PB 301 363)A05

- UCB/EERC-78/26 "Studies of Strong Ground Motion in Taiwan," by Y.M. Hsueh, B.A. Bolt and J. Penzien - 1978 (PB 296 436)A06
- UCB/EERC-78/27 "Cyclic Loading Tests of Masonry Single Piers: Volume 1 - Height to Width Ratio of 2," by P.A. Hidalgo, R.L. Mayes, H.D. McNiven and R.W. Clough - 1978 (PB 296 211)A07
- UCB/EERC-78/28 "Cyclic Loading Tests of Masonry Single Piers: Volume 2 - Height to Width Ratio of 1," by S.-W.J. Chen, P.A. Hidalgo, R.L. Mayes, R.W. Clough and H.D. McNiven - 1978 (PB 296 212)A09
- UCB/EERC-78/29 "Analytical Procedures in Soil Dynamics," by J. Lysmer - 1978 (PB 298 445)A06
- UCB/EERC-79/01 "Hysteretic Behavior of Lightweight Reinforced Concrete Beam-Column Subassemblies," by B. Forzani, E.P. Popov and V.V. Bertero - April 1979(PB 298 267)A06
- UCB/EERC-79/02 "The Development of a Mathematical Model to Predict the Flexural Response of Reinforced Concrete Beams to Cyclic Loads, Using System Identification," by J. Stanton & H. McNiven - Jan. 1979(PB 295 875)A10
- UCB/EERC-79/03 "Linear and Nonlinear Earthquake Response of Simple Torsionally Coupled Systems," by C.L. Kan and A.K. Chopra - Feb. 1979(PB 298 262)A06
- UCB/EERC-79/04 "A Mathematical Model of Masonry for Predicting its Linear Seismic Response Characteristics," by Y. Mengi and H.D. McNiven - Feb. 1979(PB 298 266)A06
- UCB/EERC-79/05 "Mechanical Behavior of Lightweight Concrete Confined by Different Types of Lateral Reinforcement," by M.A. Manrique, V.V. Bertero and E.P. Popov - May 1979(PB 301 114)A06
- UCB/EERC-79/06 "Static Tilt Tests of a Tall Cylindrical Liquid Storage Tank," by R.W. Clough and A. Niwa - Feb. 1979 (PB 301 167)A06
- UCB/EERC-79/07 "The Design of Steel Energy Absorbing Restrainers and Their Incorporation into Nuclear Power Plants for Enhanced Safety: Volume 1 - Summary Report," by R.N. Spencer, V.F. Zackay, and E.R. Parker - Feb. 1979(UCB/EERC-79/07)A09
- UCB/EERC-79/08 "The Design of Steel Energy Absorbing Restrainers and Their Incorporation into Nuclear Power Plants for Enhanced Safety: Volume 2 - The Development of Analyses for Reactor System Piping," "Simple Systems" by M.C. Lee, J. Penzien, A.K. Chopra and K. Suzuki "Complex Systems" by G.H. Powell, E.C. Wilson, R.W. Clough and D.D. Row - Feb. 1979(UCB/EERC-79/08)A11
- UCB/EERC-79/09 "The Design of Steel Energy Absorbing Restrainers and Their Incorporation into Nuclear Power Plants for Enhanced Safety: Volume 3 - Evaluation of Commercial Steels," by W.S. Owen, R.M.N. Pelloux, R.J. Ritchie, M. Faral, T. Ohhashi, J. Toplosky, S.J. Hartman, V.F. Zackay and E.R. Parker - Feb. 1979(UCB/EERC-79/09)A04
- UCB/EERC-79/10 "The Design of Steel Energy Absorbing Restrainers and Their Incorporation into Nuclear Power Plants for Enhanced Safety: Volume 4 - A Review of Energy-Absorbing Devices," by J.M. Kelly and M.S. Skinner - Feb. 1979(UCB/EERC-79/10)A04
- UCB/EERC-79/11 "Conservatism in Summation Rules for Closely Spaced Modes," by J.M. Kelly and J.L. Sackman - May 1979(PB 301 328)A03
- UCB/EERC-79/12 "Cyclic Loading Tests of Masonry Single Piers: Volume 3 - Height to Width Ratio of 0.5," by P.A. Hidalgo, R.L. Mayes, H.D. McNiven and R.W. Clough - May 1979(PB 301 321)A08
- UCB/EERC-79/13 "Cyclic Behavior of Dense Course-Grained Materials in Relation to the Seismic Stability of Dams," by N.G. Banerjee, H.B. Seed and C.K. Chan - June 1979(PB 301 373)A13
- UCB/EERC-79/14 "Seismic Behavior of Reinforced Concrete Interior Beam-Column Subassemblies," by S. Vivathanatepa, E.P. Popov and V.V. Bertero - June 1979(PB 301 326)A10
- UCB/EERC-79/15 "Optimal Design of Localized Nonlinear Systems with Dual Performance Criteria Under Earthquake Excitations," by M.A. Bhatti - July 1979(PB 80 167 109)A06
- UCB/EERC-79/16 "OPTDYN - A General Purpose Optimization Program for Problems with or without Dynamic Constraints," by M.A. Bhatti, E. Polak and K.S. Pister - July 1979(PB 80 167 091)A05
- UCB/EERC-79/17 "ANSR-II, Analysis of Nonlinear Structural Response, Users Manual," by C.P. Mondkar and G.H. Powell July 1979 (PB 80 113 301)A05
- UCB/EERC-79/18 "Soil Structure Interaction in Different Seismic Environments," A. Gomez-Masso, J. Lysmer, J.-C. Chen and H.B. Seed - August 1979(PB 80 101 520)A04
- UCB/EERC-79/19 "ARMA Models for Earthquake Ground Motions," by M.K. Chang, J.W. Kwiatkowski, R.F. Nau, R.M. Oliver and K.S. Pister - July 1979(PB 301 166)A05
- UCB/EERC-79/20 "Hysteretic Behavior of Reinforced Concrete Structural Walls," by J.M. Vallenat, V.V. Bertero and E.P. Popov - August 1979(PB 80 165 905)A12
- UCB/EERC-79/21 "Studies on High-Frequency Vibrations of Buildings - 1: The Column Effect," by J. Lubliner - August 1979 (PB 80 158 553)A03
- UCB/EERC-79/22 "Effects of Generalized Loadings on Bond Reinforcing Bars Embedded in Confined Concrete Blocks," by S. Vivathanatepa, E.P. Popov and V.V. Bertero - August 1979(PB 81 124 018)A14
- UCB/EERC-79/23 "Shaking Table Study of Single-Story Masonry Houses, Volume 1: Test Structures 1 and 2," by P. Gülkan, R.L. Mayes and R.W. Clough - Sept. 1979 (HUD-000 1763)A12
- UCB/EERC-79/24 "Shaking Table Study of Single-Story Masonry Houses, Volume 2: Test Structures 3 and 4," by P. Gülkan, R.L. Mayes and R.W. Clough - Sept. 1979 (HUD-000 1836)A12
- UCB/EERC-79/25 "Shaking Table Study of Single-Story Masonry Houses, Volume 3: Summary, Conclusions and Recommendations," by R.W. Clough, R.L. Mayes and P. Gülkan - Sept. 1979 (HUD-000 1837)A06

- UCB/EERC-79/26 "Recommendations for a U.S.-Japan Cooperative Research Program Utilizing Large-Scale Testing Facilities," by U.S.-Japan Planning Group - Sept. 1979(PB 301 107)A06
- UCB/EERC-79/27 "Earthquake-Induced Liquefaction Near Lake Amatitlan, Guatemala," by H.B. Seed, I. Arango, C.K. Chan, A. Jomez-Masso and R. Grant de Ascoli - Sept. 1979(NUREG-CR1341)A03
- UCB/EERC-79/28 "Infill Panels: Their Influence on Seismic Response of Buildings," by J.W. Axley and V.V. Bertero Sept. 1979(PB 80 163 371)A10
- UCB/EERC-79/29 "3D Truss Bar Element (Type 1) for the ANSR-II Program," by D.P. Mondkar and G.H. Powell - Nov. 1979 (PB 80 169 709)A02
- UCB/EERC-79/30 "2D Beam-Column Element (Type 5 - Parallel Element Theory) for the ANSR-II Program," by D.G. Row, G.H. Powell and D.P. Mondkar - Dec. 1979(PB 80 167 224)A03
- UCB/EERC-79/31 "3D Beam-Column Element (Type 2 - Parallel Element Theory) for the ANSR-II Program," by A. Rahi, G.H. Powell and D.P. Mondkar - Dec. 1979(PB 80 167 216)A03
- UCB/EERC-79/32 "On Response of Structures to Stationary Excitation," by A. Der Kiureghian - Dec. 1979(PB 80166 929)A03
- UCB/EERC-79/33 "Undisturbed Sampling and Cyclic Load Testing of Sands," by S. Singh, H.B. Seed and C.K. Chan Dec. 1979(ADA 087 298)A07
- UCB/EERC-79/34 "Interaction Effects of Simultaneous Torsional and Compressional Cyclic Loading of Sand," by P.M. Griffin and W.H. Houston - Dec. 1979(ADA 092 352)A15
- UCB/EERC-80/01 "Earthquake Response of Concrete Gravity Dams Including Hydrodynamic and Foundation Interaction Effects," by A.K. Chopra, P. Enkrabarti and S. Gupta - Jan. 1980(AD-A087297)A10
- UCB/EERC-80/02 "Rocking Response of Rigid Blocks to Earthquakes," by C.S. Yam, A.K. Chopra and J. Penzien - Jan. 1980 (PB80 166 102)A04
- UCB/EERC-80/03 "Optimum Inelastic Design of Seismic-Resistant Reinforced Concrete Frame Structures," by S.W. Zagajski and V.V. Bertero - Jan. 1980(PB80 164 635)A06
- UCB/EERC-80/04 "Effects of Amount and Arrangement of Wall-Panel Reinforcement on Hysteretic Behavior of Reinforced Concrete Walls," by R. Ilyas and V.V. Bertero - Feb. 1980(PB81 122 525)A09
- UCB/EERC-80/05 "Shaking Table Research on Concrete Dam Models," by A. Niwa and R.W. Clough - Sept. 1980(PB81 122 368)A06
- UCB/EERC-80/06 "The Design of Steel Energy-Absorbing Restrainers and their Incorporation into Nuclear Power Plants for Enhanced Safety (Vol 1A): Piping with Energy Absorbing Restrainers: Parameter Study on Small Systems," by G.H. Powell, C. Coughourlian and J. Simons - June 1980
- UCB/EERC-80/07 "Inelastic Torsional Response of Structures Subjected to Earthquake Ground Motions," by Y. Yamazaki April 1980(PB81 122 327)A08
- UCB/EERC-80/08 "Study of X-Braced Steel Frame Structures Under Earthquake Simulation," by Y. Ghaemat - April 1980 (PB81 122 335)A11
- UCB/EERC-80/09 "Hybrid Modelling of Soil-Structure Interaction," by S. Gupta, T.W. Lin, J. Penzien and C.S. Yeh May 1980(PB81 122 319)A07
- UCB/EERC-80/10 "General Applicability of a Nonlinear Model of a One Story Steel Frame," by B.I. Sveinsson and H.D. McInven - May 1980(PB81 124 377)A06
- UCB/EERC-80/11 "A Green-Function Method for Wave Interaction with a Submerged Body," by W. Kioka - April 1980 (PB81 122 269)A07
- UCB/EERC-80/12 "Hydrodynamic Pressure and Added Mass for Axisymmetric Bodies," by F. Nairat - May 1980(PB81 122 343)A08
- UCB/EERC-80/13 "Treatment of Non-Linear Drag Forces Acting on Offshore Platforms," by B.V. Dao and J. Penzien May 1980(PB81 153 413)A07
- UCB/EERC-80/14 "2D Plane/Axisymmetric Solid Element (Type 3 - Elastic or Elastic-Perfectly Plastic) for the ANSR-II Program," by D.P. Mondkar and G.H. Powell - July 1980(PB81 122 350)A03
- UCB/EERC-80/15 "A Response Spectrum Method for Random Vibrations," by A. Der Kiureghian - June 1980(PB81 122 301)A03
- UCB/EERC-80/16 "Cyclic Inelastic Buckling of Tubular Steel Braces," by V.A. Zayas, E.P. Popov and S.A. Mahin June 1980(PB81 124 985)A10
- UCB/EERC-80/17 "Dynamic Response of Simple Arch Dams Including Hydrodynamic Interaction," by C.S. Porter and A.K. Chopra - July 1980(PB81 124 000)A13
- UCB/EERC-80/18 "Experimental Testing of a Friction Damped Aseismic Base Isolation System with Fail-Safe Characteristics," by J.M. Kelly, K.E. Baucke and M.S. Skinner - July 1980(PB81 148 595)A04
- UCB/EERC-80/19 "The Design of Steel Energy-Absorbing Restrainers and their Incorporation into Nuclear Power Plants for Enhanced Safety (Vol 1B): Stochastic Seismic Analysis of Nuclear Power Plant Structures and Piping Systems Subjected to Multiple Support Excitations," by M.C. Lee and J. Penzien - June 1980
- UCB/EERC-80/20 "The Design of Steel Energy-Absorbing Restrainers and their Incorporation into Nuclear Power Plants for Enhanced Safety (Vol 1C): Numerical Method for Dynamic Substructure Analysis," by J.M. Dickens and E.L. Wilson - June 1980
- UCB/EERC-80/21 "The Design of Steel Energy-Absorbing Restrainers and their Incorporation into Nuclear Power Plants for Enhanced Safety (Vol 2): Development and Testing of Restraints for Nuclear Piping Systems," by J.M. Kelly and M.S. Skinner - June 1980
- UCB/EERC-80/22 "3D Solid Element (Type 4-Elastic or Elastic-Perfectly-Plastic) for the ANSR-II Program," by D.P. Mondkar and G.H. Powell - July 1980(PB81 123 242)A03
- UCB/EERC-80/23 "Gap-Friction Element (Type 5) for the ANSR-II Program," by D.P. Mondkar and G.H. Powell - July 1980 (PB81 122 285)A03

- UCB/EERC-80/24 "U-Bar Restraint Element (Type 11) for the ANSR-II Program," by C. Oughourlian and G.H. Powell July 1980(PB81 122 293)A03
- UCB/EERC-80/25 "Testing of a Natural Rubber Base Isolation System by an Explosively Simulated Earthquake," by J.M. Kelly - August 1980(PB81 201 360)A04
- UCB/EERC-80/26 "Input Identification from Structural Vibrational Response," by Y. Hu - August 1980(PB81 152 308)A05
- UCB/EERC-80/27 "Cyclic Inelastic Behavior of Steel Offshore Structures," by V.A. Zayas, S.A. Mahin and E.P. Popov August 1980(PB81 136 180)A15
- UCB/EERC-80/28 "Shaking Table Testing of a Reinforced Concrete Frame with Biaxial Response," by M.G. Olive October 1980(PB81 154 304)A13
- UCB/EERC-80/29 "Dynamic Properties of a Twelve-Story Prefabricated Panel Building," by J.G. Bouwkamp, J.P. Kollegger and R.M. Stephen - October 1980(PB82 117 128)A06
- UCB/EERC-80/30 "Dynamic Properties of an Eight-Story Prefabricated Panel Building," by J.G. Bouwkamp, J.P. Kollegger and R.M. Stephen - October 1980(PB81 200 313)A05
- UCB/EERC-80/31 "Predictive Dynamic Response of Panel Type Structures Under Earthquakes," by J.P. Kollegger and J.G. Bouwkamp - October 1980(PB81 316)A04
- UCB/EERC-80/32 "The Design of Steel Energy-Absorbing Restrainers and their Incorporation into Nuclear Power Plants for Enhanced Safety (Vol 3): Testing of Commercial Steels in Low-Cycle Torsional Fatigue," by P. Spencer, E.R. Parker, E. Tongewaard and M. Drozy
- UCB/EERC-80/33 "The Design of Steel Energy-Absorbing Restrainers and their Incorporation into Nuclear Power Plants for Enhanced Safety (Vol 4): Shaking Table Tests of Piping Systems with Energy-Absorbing Restrainers," by S.F. Stiemer and W.G. Godden - Sept. 1980
- UCB/EERC-80/34 "The Design of Steel Energy-Absorbing Restrainers and their Incorporation into Nuclear Power Plants for Enhanced Safety (Vol 5): Summary Report," by P. Spencer
- UCB/EERC-80/35 "Experimental Testing of an Energy-Absorbing Base Isolation System," by J.M. Kelly, M.S. Skinner and A.E. Beucke - October 1980(PB81 154 072)A04
- UCB/EERC-80/36 "Simulating and Analyzing Artificial Non-Stationary Earthquake Ground Motions," by R.F. Nau, R.M. Oliver and K.S. Pister - October 1980(PB81 153 297)A04
- UCB/EERC-80/37 "Earthquake Engineering at Berkeley - 1980," - Sept. 1980(PB81 205 674)A09
- UCB/EERC-80/38 "Inelastic Seismic Analysis of Large Panel Buildings," by V. Schrieker and G.H. Powell - Sept. 1980 (PB81 154 338)A13
- UCB/EERC-80/39 "Dynamic Response of Embankment, Concrete-Gravity and Arch Dams Including Hydrodynamic Interaction," by J.F. Hall and A.K. Chopra - October 1980(PB81 152 324)A12
- UCB/EERC-80/40 "Inelastic Buckling of Steel Struts Under Cyclic Load Reversal," by R.G. Black, W.A. Wenger and E.P. Popov - October 1980(PB81 154 312)A08
- UCB/EERC-80/41 "Influence of Site Characteristics on Building Damage During the October 3, 1974 Lima Earthquake," by P. Rapetto, I. Arango and H.B. Seed - Sept. 1980(PB81 161 739)A05
- UCB/EERC-80/42 "Evaluation of a Shaking Table Test Program on Response Behavior of a Two Story Reinforced Concrete Frame," by J.M. Blondet, R.W. Clough and S.A. Mahin
- UCB/EERC-80/43 "Modelling of Soil-Structure Interaction by Finite and Infinite Elements," by F. Medina - December 1980(PB81 229 270)A04
- UCB/EERC-81/01 "Control of Seismic Response of Piping Systems and Other Structures by Base Isolation," edited by J.M. Kelly - January 1981 (PB81 200 735)A05
- UCB/EERC-81/02 "OPTNSR - An Interactive Software System for Optimal Design of Statically and Dynamically Loaded Structures with Nonlinear Response," by M.A. Bhatti, V. Ciampi and K.S. Pister - January 1981 (PB81 218 851)A09
- UCB/EERC-81/03 "Analysis of Local Variations in Free Field Seismic Ground Motions," by J.-C. Chen, J. Lysmer and H.B. Seed - January 1981 (AD-A099508)A13
- UCB/EERC-81/04 "Inelastic Structural Modeling of Braced Offshore Platforms for Seismic Loading," by V.A. Zayas, P.-S.B. Shing, S.A. Mahin and E.P. Popov - January 1981(PB82 138 777)A07
- UCB/EERC-81/05 "Dynamic Response of Light Equipment in Structures," by A. Der Kiureghian, J.L. Sackman and B. Nour-Omid - April 1981 (PB81 218 497)A04
- UCB/EERC-81/06 "Preliminary Experimental Investigation of a Broad Base Liquid Storage Tank," by J.G. Bouwkamp, J.P. Kollegger and R.M. Stephen - May 1981(PB82 140 385)A03
- UCB/EERC-81/07 "The Seismic Resistant Design of Reinforced Concrete Coupled Structural Walls," by A.E. Aktan and V.V. Bertero - June 1981(PB82 113 358)A11
- UCB/EERC-81/08 "The Undrained Shearing Resistance of Cohesive Soils at Large Deformations," by M.R. Pyles and H.B. Seed - August 1981
- UCB/EERC-81/09 "Experimental Behavior of a Spatial Piping System with Steel Energy Absorbers Subjected to a Simulated Differential Seismic Input," by S.F. Stiemer, W.G. Godden and J.M. Kelly - July 1981

- UCB/EERC-81/10 "Evaluation of Seismic Design Provisions for Masonry in the United States," by B.T. Swainson, R.D. Maves and H.D. McNiven - August 1981
- UCB/EERC-81/11 "Two-Dimensional Hybrid Modelling of Soil-Structure Interaction," by I.-J. Tzong, S. Gupta and J. Penzien - August 1981 (PB82 140 106) A04
- UCB/EERC-81/12 "Studies on Effects of Infills in Seismic Resistant R/C Construction," by S. Frkkan and V.V. Bertero - September 1981
- UCB/EERC-81/13 "Linear Models to Predict the Nonlinear Seismic Behavior of a One-Story Steel Frame," by H. Valdimarsson, A.H. Shah and H.D. McNiven - September 1981 (PB82 138 791) A07
- UCB/EERC-81/14 "TLUSH: A Computer Program for the Three-Dimensional Dynamic Analysis of Earth Dams," by T. Kagawa, L.H. Meija, H.B. Seed and J. Lysmer - September 1981 (PB82 139 940) A06
- UCB/EERC-81 15 "Three Dimensional Dynamic Response Analysis of Earth Dams," by L.H. Meija and H.B. Seed - September 1981 (PB82 137 274) A12
- UCB/EERC-81 16 "Experimental Study of Lead and Elastomeric Dampers for Base Isolation Systems," by J.M. Kelly and S.B. Hodder - October 1981
- UCB/EERC-81 17 "The Influence of Base Isolation on the Seismic Response of Light Secondary Equipment," by J.M. Kelly - April 1981
- UCB/EERC-81 18 "Studies on Evaluation of Shaking Table Response Analysis Procedures," by J. Marcial Blondet - November 1981
- UCB/EERC-81 19 "DELIGHT.STRUCT: A Computer-Aided Design Environment for Structural Engineering," by R.J. Balling, K.S. Pister and E. Polak - December 1981
- UCB/EERC-81 20 "Optimal Design of Seismic-Resistant Planar Steel Frames," by R.J. Balling, V. Ciampi, K.S. Pister and E. Polak - December 1981
- UCB/EERC-82/01 "Dynamic Behavior of Ground for Seismic Analysis of Lifeline Systems," by T. Sato and A. Der Kiureghian - January 1982 (PB82 218 926) A05
- UCB/EERC-82/02 "Shaking Table Tests of a Tubular Steel Frame Model," by Y. Ghanaat and R. W. Clough - January 1982 (PB82 220 161) A07
- UCB/EERC-82/03 "Experimental Behavior of a Spatial Piping System with Shock Arrestors and Energy Absorbers under Seismic Excitation," by S. Schneider, H.-M. Lee and G. W. Godden - May 1982
- UCB/EERC-82/04 "New Approaches for the Dynamic Analysis of Large Structural Systems," by E. L. Wilson - June 1982
- UCB/EERC-82/05 "Model Study of Effects on the Vibration Properties of Steel Offshore Platforms," by F. Shahriyar and J. G. Bouwkamp - June 1982
- UCB/EERC-82/06 "States of the Art and Practice in the Optimum Seismic Design and Analytical Response Prediction of R/C Frame-Wall Structures," by A. E. Aktan and V. V. Bertero - July 1982
- UCB/EERC-82/07 "Further Study of the Earthquake Response of a Broad Cylindrical Liquid-Storage Tank Model," by G. C. Manos and R. W. Clough - July 1982
- UCB/EERC-82/08 "An Evaluation of the Design and Analytical Seismic Response of a Seven Story Reinforced Concrete Frame - Wall Structure," by A. C. Finley and V. V. Bertero - July 1982
- UCB/EERC-82/09 "Fluid-Structure Interactions: Added Mass Computations for Incompressible Fluid," by J. S.-H. Kuo - August 1982
- UCB/EERC-82/10 "Joint-Opening Nonlinear Mechanism: Interface Smeared Crack Model," by J. S.-H. Kuo - August 1982

- UCB/EERC-82/11 "Dynamic Response Analysis of Tachi Dam," by R. W. Clough, R. M. Stephen and J. S.-H. Kuo - August 1982
- UCB/EERC-82/12 "Prediction of the Seismic Responses of R/C Frame-Coupled Wall Structures," by A. E. Aktan, V. V. Bertero and M. Piazza - August 1982
- UCB/EERC-82/13 "Preliminary Report on the SMART 1 Strong Motion Array in Taiwan," by B. A. Bolt, C. H. Loh, J. Penzien, Y. B. Tsai and Y. T. Yeh - August 1982
- UCB/EERC-82/14 "Shaking-Table Studies of an Eccentrically X-Braced Steel Structure," by M. S. Yang - September 1982
- UCB/EERC-82/15 "The Performance of Stairways in Earthquakes," by C. Roha, J. W. Axley and V. V. Bertero - September 1982
- UCB/EERC-82/16 "The Behavior of Submerged Multiple Bodies in Earthquakes," by W.-J. Liao - September 1982
- UCB/EERC-82/17 "Effects of Concrete Types and Loading Conditions on Local Bond-Slip Relationships," by A. D. Cowell, E. P. Popov and V. V. Bertero - September 1982
- UCB/EERC-82/18 "Mechanical Behavior of Shear Wall Vertical Boundary Members: An Experimental Investigation," by Maryann T. Wagner and Vitelmo V. Bertero - October 1982